


Spring 4-28-2021

Thermal, Mechanical, and Rehealing Properties of Cross-linked Ionene Networks

Katelyn Lindenmeyer

Follow this and additional works at: <https://digitalcommons.murraystate.edu/honorsthesis>

 Part of the [Materials Chemistry Commons](#), [Organic Chemistry Commons](#), and the [Polymer Chemistry Commons](#)

Recommended Citation

Lindenmeyer, Katelyn, "Thermal, Mechanical, and Rehealing Properties of Cross-linked Ionene Networks" (2021). *Honors College Theses*. 74.

<https://digitalcommons.murraystate.edu/honorsthesis/74>

This Thesis is brought to you for free and open access by the Honors College at Murray State's Digital Commons. It has been accepted for inclusion in Honors College Theses by an authorized administrator of Murray State's Digital Commons. For more information, please contact msu.digitalcommons@murraystate.edu.

Murray State University Honors College

HONORS THESIS

Certificate of Approval

Thermal, Mechanical, and Rehealing properties of Cross-linked Ionene Networks

Katelyn Lindenmeyer

May 2021

Approved to fulfill the
requirements of HON 437

Dr. Kevin Miller, Professor
Chemistry

Approved to fulfill the
Honors Thesis requirement
of the Murray State Honors
Diploma

Dr. Warren Edminster, Executive Director
Honors College

Examination Approval Page

Author: Katelyn Lindenmeyer

Project Title: Thermal, Mechanical, and Rehealing properties of Cross-linked Ionene Networks

Department: Chemistry

Date of Defense: April 28, 2021

Approval by Examining Committee:

(Dr. Kevin Miller, Advisor)

(Date)

(Dr. Daniel Johnson, Committee Member)

(Date)

(Dr. Grace Eder, Committee Member)

(Date)

Thermal, Mechanical, and Rehealing properties of Cross-linked Ionene Networks

Submitted in partial fulfillment
of the requirements
for the Murray State University Honors Diploma

Katelyn Lindenmeyer

May 2021

Table of Contents

List of Schemes	i
List of Figures	ii
List of Tables	iv
Abstract	v
Chapter 1: Introduction and Project Scope	1
1.1 Ion Containing Polymers	1
1.2 Covalent Adaptable Networks	4
1.3 Covalently Crosslinked Ionene Networks and Photopolymerization	8
Chapter 2: Self-Healing behavior of Furan Maleimide Poly(ionic liquid) Covalent Adaptable Networks	11
2.1 Overview	11
2.2 Results and Discussion	12
2.3 Experimental	16
2.3.1 Materials	16
2.3.2 Synthesis of Mono-imidazolium Maleimide [NTf ₂] monomer	17
2.3.3 Synthesis of Bisimidazolium Maleimide [NTf ₂] monomer	19
2.3.4 Synthesis of PIL-CAN-IM/PIL-CAN-IM2	20
2.3.5 Monomer Characterization	20
2.3.6 Polymer Characterization	21
2.3.7 Rehealing Studies	22
2.4 Summary	22
Chapter 3: Synthesis, Thermal and Mechanical Properties of Imidazolium Containing Thiol-yne Ionene Networks	24
3.1 Overview	24
3.2 Results and Discussion	27
3.2.1 Monomer Synthesis	27
3.2.3 Synthesis of Ionene Networks	28
3.2.3 Thermal Properties	29

3.2.4 Mechanical Properties	30
3.2.5 Photorheology	33
3.3 Experimental	34
3.3.1 General	34
3.3.2 Synthesis of 6-Iodo-1-hexyne	35
3.3.3 Synthesis of <i>N</i> -(6-hexynyl) imidazole	35
3.3.4 Synthesis of bis(6-hexynyl) imidazolium chloride	36
3.3.5 Synthesis of bis(6-hexynyl) imidazolium [NTf ₂]	36
3.3.6 Polymer Synthesis	37
3.3.7 Polymer Characterization	37
3.4 Summary	38
References	40
Supplementary Information	45

List of Schemes

Scheme 1.1: Synthesis of Poly(<i>N</i> -alkylimidazolium Acrylate)	3
Scheme 1.2: S _N 2 Polymerization of Imidazolium Ionenes	3
Scheme 1.3: Diels Alder Cycloaddition and Retro-cycloaddition Reaction for Furan and Maleimide Cycloadducts	5
Scheme 1.4: Examples of Dynamic and Reversible Cross-links in Network Polymers	6
Scheme 1.5: Diels-Alder Reaction for Reversible Covalent Bonds	7
Scheme 1.6: Scope of Michael Addition Polymerization Approach to Ionene Network Formation	8
Scheme 1.7: Mechanism of Thiol-ene “Click” Photopolymerization	9
Scheme 1.8: Synthesis of Imidazolium-Containing Thiol-ene Ionene Network	10
Scheme 2.1: Synthesis of Ruran-Protected <i>N</i> -(4-Bromobutyl)maleimide	12
Scheme 2.2: Synthesis of Mono-Imidazolium Maleimide [NTf ₂] Monomer	12
Scheme 2.3: Synthesis of Bisimidazolium Maleimide [NTf ₂] Monomer	13
Scheme 2.4: Synthesis of PIL-CAN-IM/PIL-CAN-IM2	14
Scheme 3.1: Possible Products of a Thiol-yne Photoreaction	25
Scheme 3.2: Radical Thiol-yne Reaction Mechanism	26
Scheme 3.3: Example Thiol- and -Yne Monomer Combination	27
Scheme 3.4: Synthesis of Yne-functional [NTf ₂] Monomer	28
Scheme 3.5: Synthesis of the Thiol-yne Ionene Networks	29

List of Figures

Figure 2.1: Stress-Strain Recovery Data for (top) PIL-CAN-IM and (bottom) PIL-CAN-IM2 at 105°C	15
Figure 2.2: Samples from a Representative Re-heal Stress-Strain Trial for PIL-CAN-IM at 105 °C	16
Figure 2.3: Samples from a Representative Re-heal Stress-Strain Trial for PIL-CAN-IM2 at 105 °C	16
Figure 3.1: DSC Overlay of Thiol-yne Ionene Networks	30
Figure 3.2: DMA Storage Modulus Curve Overlay of Thiol-yne Ionene Networks	31
Figure 3.3: Tan δ Overlay of Thiol-yne Ionene Networks	32
Figure 3.4: Sample Experimental Data from Photorheology of 1:1 Thiol:yne Ionene Network	34
Figure S1: ^1H NMR spectrum of MA-IM NTf ₂ 5 (DMSO- <i>d</i> ₆)	45
Figure S2: ^{13}C NMR spectrum of MA-IM NTf ₂ 5 (DMSO- <i>d</i> ₆)	45
Figure S3: ^1H NMR spectrum of MA-IM2 NTf ₂ 8 (DMSO- <i>d</i> ₆)	46
Figure S4: ^{13}C NMR spectrum of MA-IM2 NTf ₂ 8 (DMSO- <i>d</i> ₆)	46
Figure S5: Overlay of DSC Traces (1 st and 2 nd heating) for PIL-CAN-IM and PIL-CAN-IM2 Networks	47
Figure S6: Overlay of TGA Traces for PIL-CAN-IM and PIL-CAN-IM2 Networks	47
Figure S7: Overlay of DMA Curves for PIL-CAN-IM and PIL-CAN-IM2 Networks	48
Figure S8: Overlay of tan δ Curves for PIL-CAN-IM and PIL-CAN-IM2	48
Figure S9: ^1H NMR Spectrum of 6-Iodohept-1-yne (CDCl ₃)	49
Figure S10: ^1H NMR Spectrum of 6-Hexynylimidazole (CDCl ₃)	49

Figure S11: ^{13}C NMR Spectrum of 6-Hexynylimidazole (CDCl_3)	
50	
Figure S12: ^1H NMR Spectrum of Bis(6-hexynyl)imidazolium chloride ($\text{DMSO-}d_6$)	50
Figure S13: ^1H NMR Spectrum of Bis(6-hexynyl)imidazolium [NTf_2] ($\text{DMSO-}d_6$)	
51	
Figure S14: ^{13}C NMR Spectrum of Bis(6-hexynyl)imidazolium [NTf_2] ($\text{DMSO-}d_6$)	
51	

List of Tables

Table 2.1: Thermal and Mechanical Properties of PIL-CANs	14
Table 3.1: Glass Transitions Temperatures as determined by DSC	29
Table 3.2: Summary of Mechanical Properties of Thiol-yne Ionene Networks	32
Table 3.3: Summary of Gelation Times for Thiol-yne Networks	34

Abstract

Polymers which contain ionic liquid groups have numerous applications in a wide variety of fields. Past research from our group has shown that IL-containing polymers which exist in covalently crosslinked networks can exhibit good ionic conductivities despite the hindrance in polymer chain mobility and relaxation. In part one of this thesis, efforts to create ionic networks which have the capability of being rehealed after exposure to an external stimulus are discussed. Thermoreversible maleimide-furan chemistry was incorporated into an imidazolium-containing ionene network. Maleimide-terminated, imidazolium-containing monomers were coupled with furan-functionalized monomers, prepared from commercially available multifunctional acrylates. Thermal, mechanical and rheological characterization of the networks will be presented and discussed. In the second part of the thesis, the use of thiol-yne photopolymerization as a way to prepare new ionene networks is explained. A series of imidazolium-based bis(trifluoromethylsulfonyl)imide [NTf₂] ionene networks were prepared by using thiol-yne 'click' photopolymerization to crosslink bisalkynylimidazolium [NTf₂] monomers with pentaerythritol tetrakis(3-mercaptopropionate) (PTMP). The thiol:yne molar ratio was varied in order to examine changes in the thermal and mechanical properties of the resulting polymer networks. Photorheology was utilized to determine the approximate gel points for each of the polymer networks prepared. Crosslink density was the primary factor in changing glass transition temperature and tensile properties of the networks.

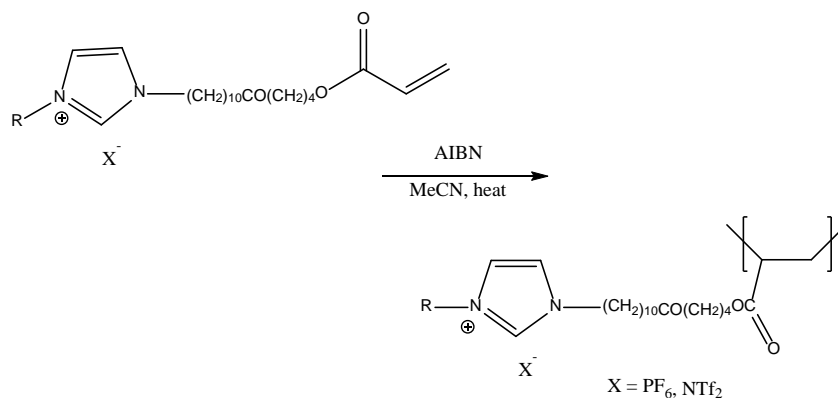
CHAPTER 1: Introduction and Project Scope

1.1: Ion-containing Polymers

Ionic liquids (IL) are salts that contain an organic cation and an organic or inorganic anion. They are used as electrolytes for improving electrochemical devices such fuel cells, batteries, drug delivery devices, and many more. However, a major issue for ILs is their mechanical instability in many of these applications. Anchoring the IL into a polymeric architecture would alleviate this issue. Ion-containing polymers can be classified into two groups: poly (ionic liquid)s and ionenes. Poly (ionic liquid)s (PILs) are ion containing polymers in which the ionic liquid group is pendant in the repeating unit of the polymer.¹⁻³ Ionenenes are ion-containing polymers in which the ionic liquid group is covalently bonded into the backbone of the polymer.⁴⁻⁶ Both of these polymers allow for variation in the macromolecular structure while retaining the characteristics of the ionic liquid monomer. Ion-containing polymers have a broad range of characteristics; they commonly have high charge densities but still maintain a broad range of glass transition temperatures (T_g), the temperature at which a glassy solid transitions to a rubbery solid. Non-network PILs are known to be soluble in a wide range of solvents, both polar and non-polar depending on the characteristics of the individual polymer. The solubility of the PIL is largely determined by the anions present.

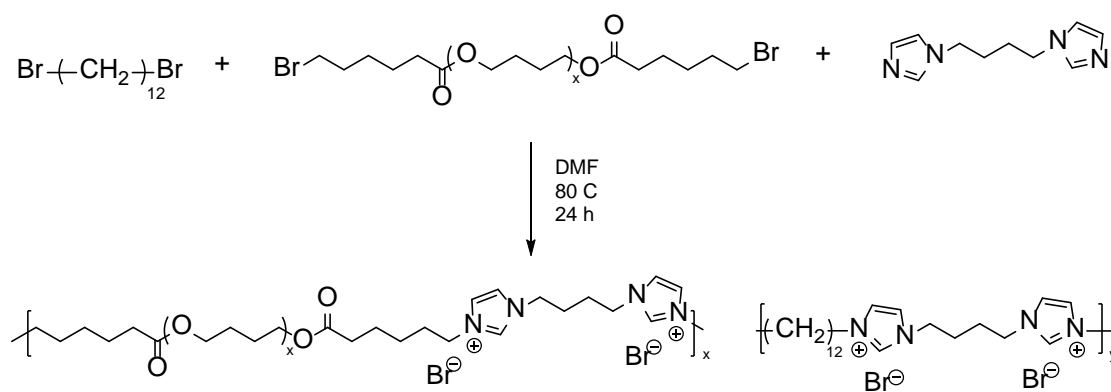
The initial uses of PILs were to enhance the functions and mechanical stability of the ionic liquid; however, their uses have grown to cover a broad range of applications and solutions. By polymerizing an ionic liquid, the valuable characteristics of the ionic liquid such as conductivity, thermal stability, and electrochemical stability are combined with polymeric attributes. This gives the ionic liquid added mechanical stability and variable viscoelasticity. This combination of useful characteristics makes ion-containing polymers a useful and broad area of study within the polymer chemistry field.

PILs can be synthesized through a various number of techniques by polymerizing a monomer containing either an anion or cation, but most commonly through free radical polymerization of a vinyl or styrenyl-substituted cationic unit (**Scheme 1.1**).⁷ The cations and anions for each poly (ionic liquid) are chosen to give a desired set of characteristics, and there are different architectures of PILs that can be created. From studies illustrating how PILs can be made from imidazolium-functionalized IL monomers, it has been hypothesized that conductivity and ion transport are mainly controlled by pendant linkage flexibility and counteranion selection. This led to several studies researching on the relationships between ionic conductivity and polymer/ion structure.⁷⁻⁹ Block copolymers have also been researched, synthesized via anionic or RAFT (reversible addition-fragmentation chain transfer) polymerization.^{4, 10, 11} These systems were found to create conductive microchannels in non-ionic block copolymers, making relatively high ionic conductivities.



Scheme 1.1: Synthesis of Poly(*N*-alkylimidazolium Acrylate).⁷

Ionenes prepared from IL- containing monomers are far less utilized. The most common strategy is the reaction between a tertiary diamine or bisimidazole and an alkyl dihalide via the Menshutkin (S_N2) reaction (**Scheme 1.2**) with a variation in linker groups.¹² Using Michael addition chemistry or thiol-ene photopolymerization, covalently crosslinked imidazolium-containing ionene networks have been created in the Miller lab.¹³⁻¹⁶ The molar ratio of the reactive functional groups was found to play a large role in determining the ductility and conductivity of the resulting ionene network.



Scheme 1.2: S_N2 Polymerization of Imidazolium Ionenes.

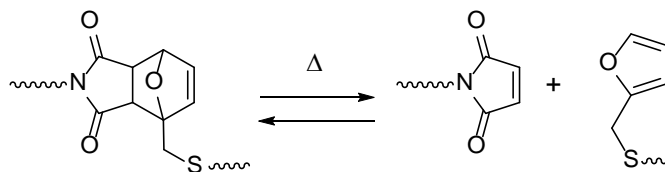
While the majority of charged polymers are focused around PILs, there is a growing research interest in ionenes. The growing interest in ionenes has encouraged more research specifically into imidazolium-based ionic liquid monomers. Imidazoles are versatile and convenient to work with compared to other cation precursors such as amines and phosphines. In this thesis two projects will be described which focus on covalently crosslinked ionene networks, one of which will contain a rehealable “dynamic” bond while the other is based upon “click” thiol-yne photopolymerization.

1.2: Covalent Adaptable Networks

Covalently-crosslinked networks, also known as thermosets, are an extensive class of elastic materials that retain their molecular structure and shape through covalent bonds which are ubiquitous throughout the network structure.¹⁷⁻²² These structures are utilized in a variety of applications ranging from composites to coatings. Though these materials are hard and have good mechanical stability, the application of various stresses can result in permanent deformation. The inclusion of dynamic covalent chemistry (reversible covalent bonding) into these networks has allowed for the reshuffling of covalent bonds to heal the damages caused by the application of a stress.²³⁻²⁶ These dynamic bonds can be chemically activated through various external stimuli including light, pH or heat. Networks such as these, that can exhibit rearrangements, are known as covalent adaptable networks.

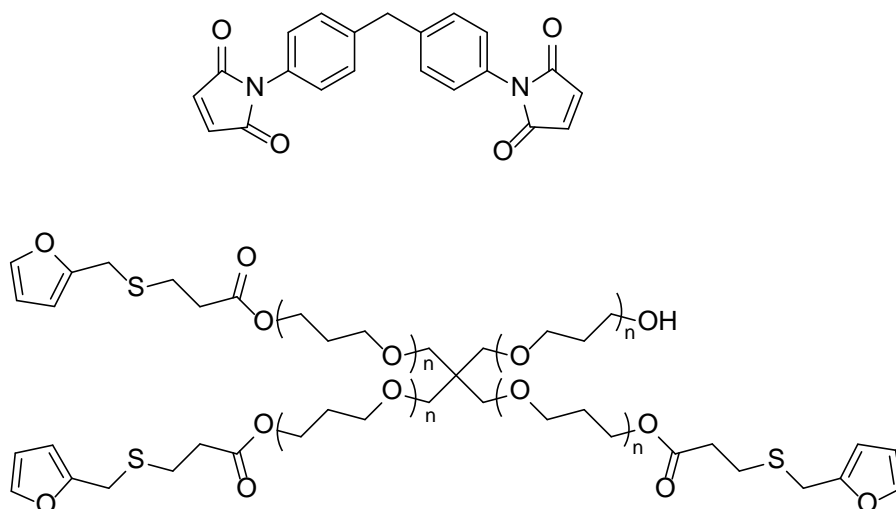
A type of dynamic covalent chemistry that is commonly used in covalent adaptable networks is the ‘click-like’ Diels-Alder cycloaddition.^{27, 28} Specifically, a furan and maleimide cycloadduct product exhibits this dynamic behavior (**Scheme 1.3**). When thermally activated, this

allows manipulation for rehealing abrasions, cracks and recycling through coupling the furan-maleimide linkage with the control at which the bond can be thermally activated.



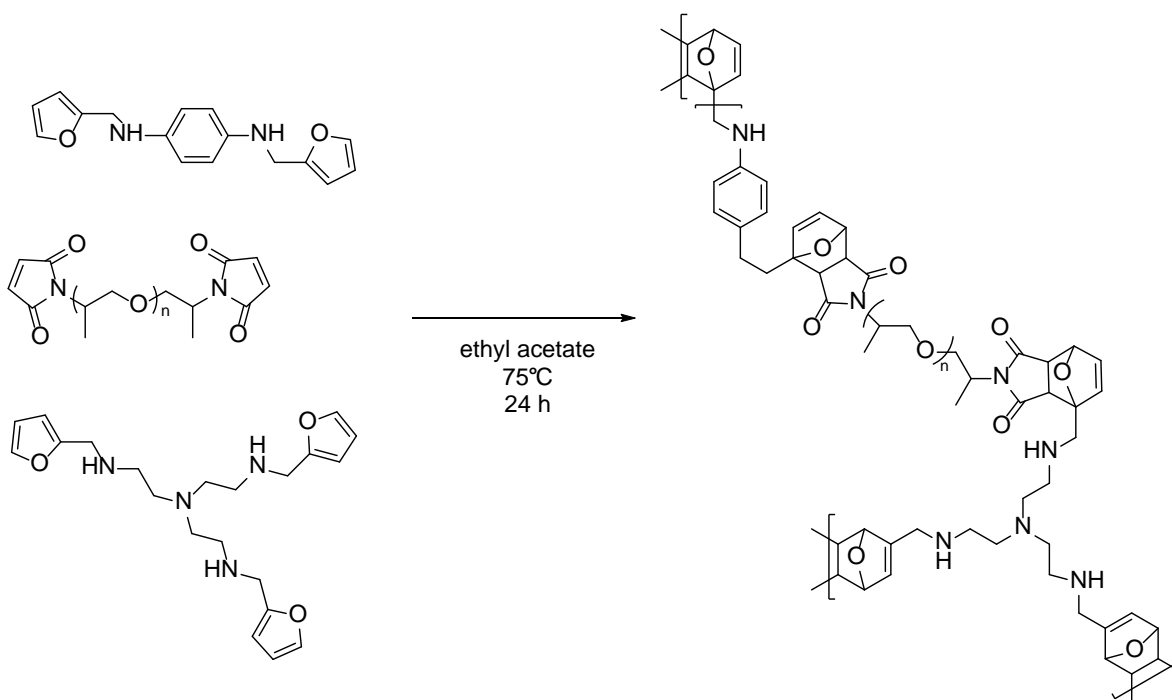
Scheme 1.3: Diels Alder Cycloaddition and Retro-cycloaddition Reaction for Furan and Maleimide Cycloadducts.

Recently, there has been a lot of interest in the applications and capabilities of covalent adaptable networks, specifically with the inclusion of Diels-Alder chemistry. A study at the University of Colorado Boulder used Diels-Alder chemistry to create dynamic and reversible cross-links in a network polymer (**Scheme 1.4**).²⁹ Characterization and analysis of this polymer showed that it exhibited significant depolymerization through the retro-Diels-Alder reaction, and low frequency relaxation due to the cross-link rearrangement.



Scheme 1.4: Examples of Dynamic and Reversible Cross-links in Network Polymers.

Another study at the University of Texas at Dallas was performed to enable functional 3D printed polymers from reversible covalent bonds formed from a Diels-Alder reaction (**Scheme 1.5**).²⁹ These polymers were found to have improved mechanical strength and toughness from the dynamic bonds; this can be used to reduce the mechanical defects incurred during the printing process.

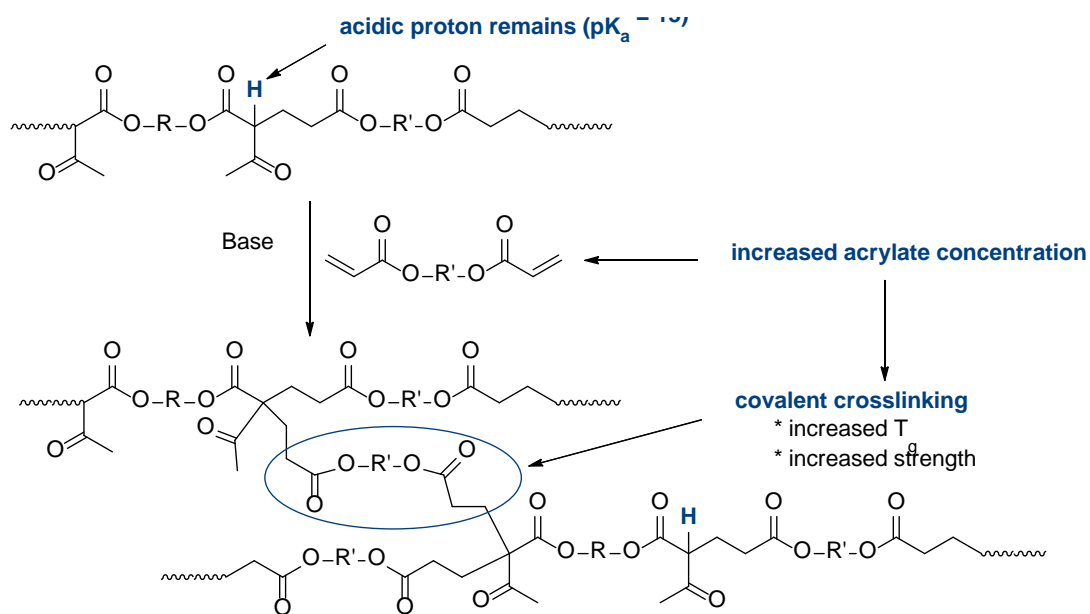


Scheme 1.5: Diels-Alder Reaction for Reversible Covalent Bonds.

The inclusion of Diels-Alder cycloaddition chemistry into covalent adaptable networks has other applications such as those explored in our lab with ion-containing polymers.²⁹ The inclusion of dynamic covalent chemistry in these networks allows for the rearrangement of covalent bonds to heal damages caused by the application of stress, which otherwise results in permanent deformation. Using furan and maleimide substituted, ion-containing monomers, dynamic bonds are created that when thermally activated can reheal abrasions made to the polymer. An additional advantage of these systems is that the backbone also contains ionic liquid groups. Thus, conductive, re-healable thermosets have been prepared. This study and its results will be discussed in Chapter 2.

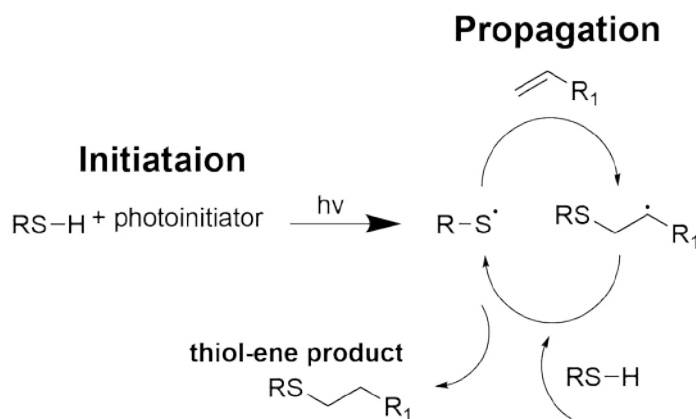
1.3: Covalently Crosslinked Ionene Networks and Photopolymerization

Covalently crosslinked networks are a broad class of elastic materials which possess the ability to maintain their molecular structure through their covalent bonds which are found throughout the structure. Since 2010, the Miller group has been very active in the development of covalently crosslinked networks which contain ionic liquid groups. Initial work focused on base-catalyzed Michael addition chemistry, creating networks from IL-containing acetoacetate monomers and commercially available multi-functional acrylates (**Scheme 1.6**).^{13, 14, 16} While this approach proved novel, the synthesis of these monomers was very difficult, thus other more efficient chemical methods to prepare ionene networks were then explored.



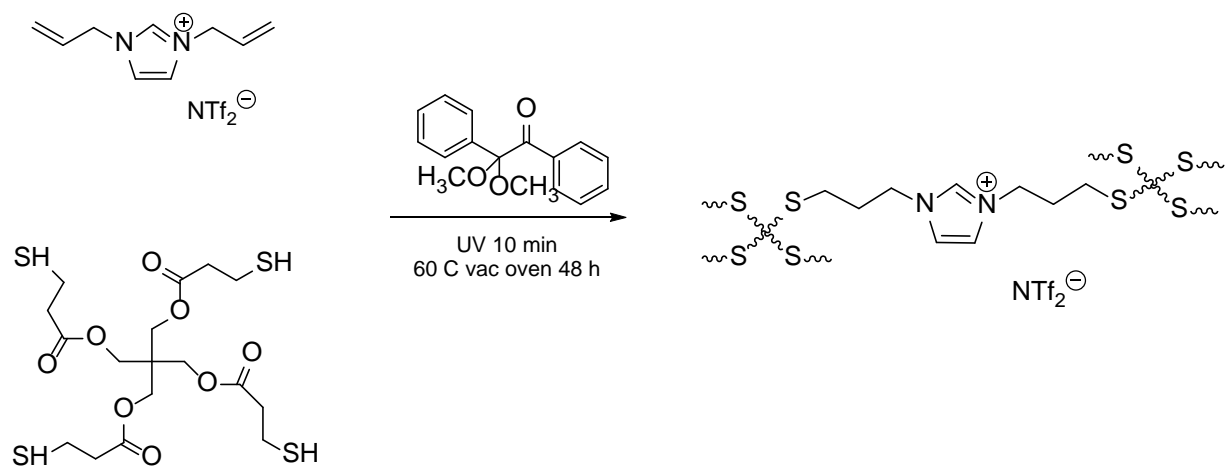
Scheme 1.6: Scope of Michael Addition Polymerization Approach to Ionene Network Formation.

A more atom-efficient approach is the ‘click like’ thiol-ene photopolymerization. The Miller group has utilized thiol-ene photopolymerization as a way to create novel ionene networks by incorporating an ionic liquid group into a multifunctional ene monomers.¹⁶ The mechanism by which the thiol-ene “click” photopolymerization occurs is a free-radical reaction with an initiation and propagation step. The thiol radical attacks the double bond of the alkene; the free radical then abstracts a hydrogen from another thiol, forming the thiol-ene product and continuing the propagation cycle (**Scheme 1.7**).



Scheme 1.7: Mechanism of Thiol-ene “Click” Photopolymerization.

Initial polymerizations were carried out at a variety of thiol:ene functional group ratios. An imidazolium containing ene monomer was reacted with PTMP and 1% DMPA (dimethylol propionic acid) photoinitiator. The solution was then UV irradiated producing transparent films. Conductivity was found to be related to both IL-group content and cross-link density. In other words, ionic conductivity was the highest when IL-group content was high while cross-link density was low.



Scheme 1.8: Synthesis of Imidazolium-Containing Thiol-ene Ionene Network.

Due to the success of the thiol-ene photopolymerizations, our group next turned its attention to thiol-yne chemistry. As each alkyne contains two π bonds, it can react with two thiol groups, leading to hyperconjugated networks. In Chapter 3, the synthesis of alkyne-terminated, IL-monomers and the corresponding crosslinked ionene networks are discussed. Correlations between thiol:yne functional group ratios with thermal and mechanical properties are also presented.

Chapter 2: Self-Healing Behavior of Furan-Maleimide Poly(ionic liquid) Covalent Adaptable Networks

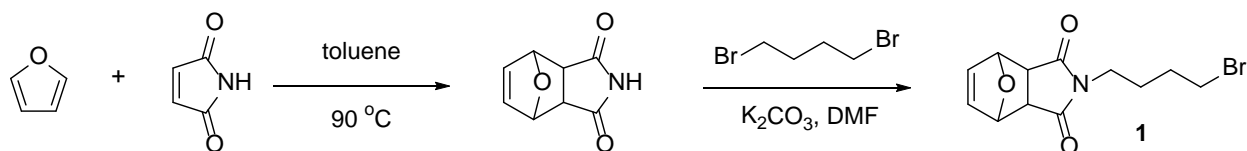
2.1: Overview

Covalent adaptable networks (CANs) are characterized by possessing dynamic properties making them ideal for a variety of applications. The inclusion of dynamic covalent chemistry, such as Diels-Alder cycloaddition into these networks allows for the rearrangement of covalent bonds to heal damages caused by the application of stress. Diels-Alder cycloaddition products are formed through the reaction between conjugated dienes and alkenes to create a cycloadduct. These newly created networks, when polymerized with an ionic liquid group, exhibit the ability to heal themselves and regain mechanical and conductive properties at rates upward of 70% when exposed to an external stimulus such as elevated temperatures.

Here, the synthesis of self-healing polymers was achieved through imidazolium containing poly(ionic liquid) covalent adaptable networks.³⁰ Recovery of mechanical and conductive properties were exhibited through the thermoreversible furan-maleimide linkages with exposure to elevated temperatures. Through dynamic mechanical analysis tensile testing, mechanical property recovery exceeding 70% was achieved after two hours at 105°C. Over longer periods of time, recovery up to 90% could be achieved. When placed between two copper electrodes for two

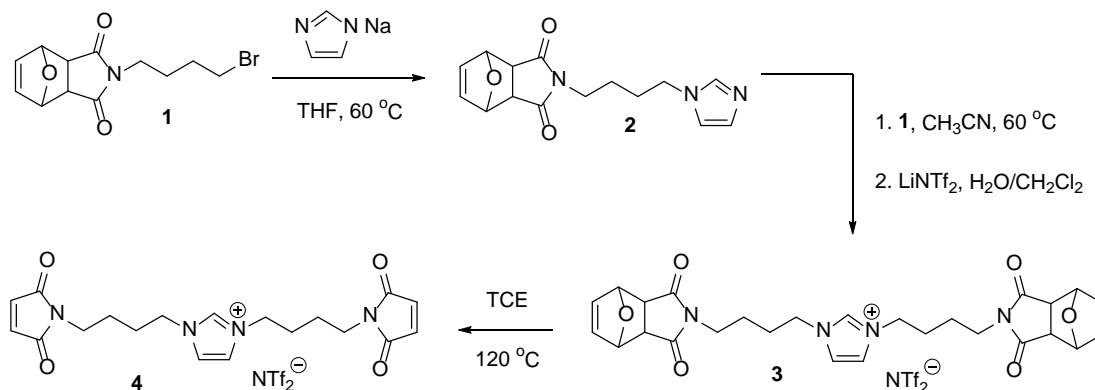
hours at 110°C, a conductivity recovery greater than 75% was exhibited after being completely severed with a razor blade.

2.2: Results and Discussion



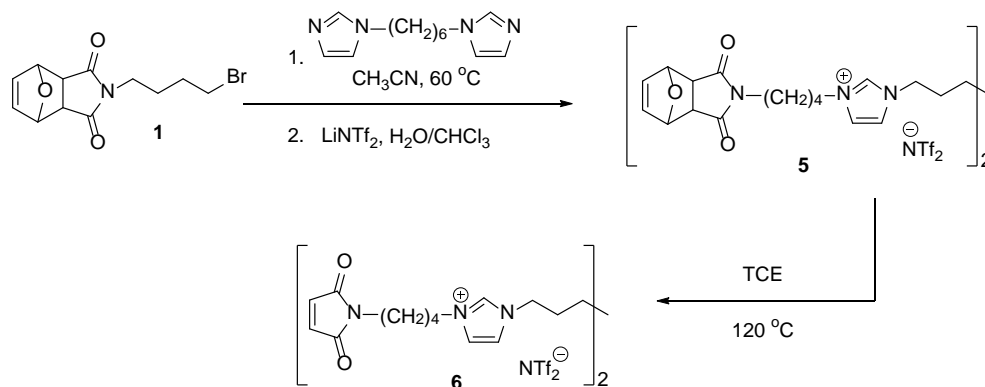
Scheme 2.1: Synthesis of Ruran-Protected *N*-(4-Bromobutyl)maleimide **1**.

The maleimide [NTf₂] monomer was synthesized using a S_N2 coupling approach. Furan-protected *N*-(4-bromobutyl)maleimide **1**³¹ (synthesis shown in **Scheme 2.1**) was coupled with sodium imidazole in tetrahydrofuran at 60 °C to give furan-protected *N*-(4-imidazolyl butyl maleimide) **2** as shown in **Scheme 2.2**. An additional mole of furan-protected *N*-(4-bromobutyl)maleimide was coupled with this product, and an ion exchange reaction with lithium bis(trifluoromethanesulfonyl)imide (LiNTf₂) was completed to produce furan-protected imidazolium [NTf₂] salt **3**. The final maleimide [NTf₂] monomer **4** was isolated by deprotection of furan at 120 °C in tetrachloroethane (TCE).



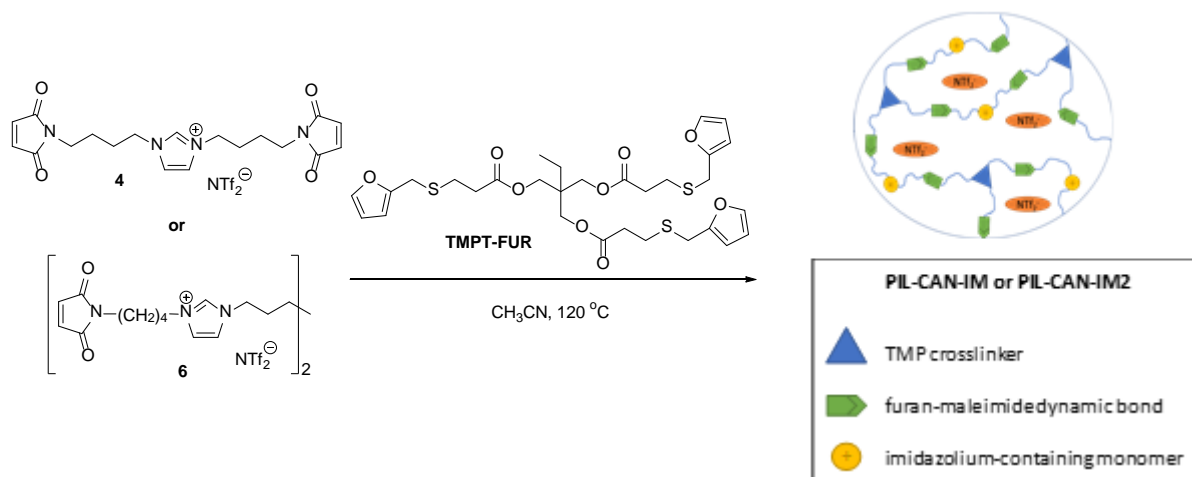
Scheme 2.2: Synthesis of Mono-Imidazolium Maleimide [NTf₂] Monomer.

Synthesis of the target bisimidazolium monomer was achieved by first reacting two moles of furan-protected *N*-(4-bromobutyl)maleimide **1** with 1,6-bisimidazolylhexane (**Scheme 2.3**). This product underwent a subsequent ion exchange using LiNTf₂ to exchange the existing bromide anion to a NTf₂ anion. Deprotection of furan was accomplished in tetrachloroethane at 120 °C to give the final bisimidazolium maleimide [NTf₂] monomer **6**.



Scheme 2.3: Synthesis of Bisimidazolium Maleimide [NTf₂] Monomer.

Synthesis of the PIL-CAN-IM or PIL-CAN-IM2 polymer networks was achieved by taking the corresponding mono- or bisimidazole maleimide monomer, and combining it in a 1:1 ratio with the furan-functionalized crosslinker TMPT-FUR in CH₃CN (**Scheme 2.4**). The resulting solution was poured into a TeflonTM mold with a glass bottom and allowed to cure in a convection oven at 120 °C for 60 minutes. The solvent was also evaporated during this time. The resulting films were clear with varying degrees of dark red color and a brittle feel to them.



Scheme 2.4: Synthesis of PIL-CAN-IM/PIL-CAN-IM2.

The storage modulus (E') was determined for each PIL-CAN using dynamic mechanical analysis (**Table 2.1**). A higher rubbery plateau modulus was exhibited in PIL-CAN-IM (1.50 MPa at $80\text{ }^\circ\text{C}$) compared to PIL-CAN-IM2 (0.66 MPa at $80\text{ }^\circ\text{C}$); this indicates a higher crosslink density. Differential scanning calorimetry was used to determine the glass transition temperature (T_g), which is the temperature at which the polymer transitions from a rigid glassy material to a soft material. It was determined that PIL-CAN-IM exhibited a higher T_g ($12.8\text{ }^\circ\text{C}$) than PIL-CAN-IM2 ($2.5\text{ }^\circ\text{C}$) (Figure S5); this is due to higher crosslink density in the PIL-CAN-IM system. Thermogravimetric analysis (TGA) was used to determine that both networks exhibit thermal stability ($T_{d5\%}$), which is the 5% thermal decomposition temperature, up to $275\text{ }^\circ\text{C}$.

Table 2.1: Thermal and Mechanical Properties of PIL-CANs.

	DSC T_g ($^\circ\text{C}$)	TGA $T_{d5\%}$ ($^\circ\text{C}$)	DMA E' @ $80\text{ }^\circ\text{C}$ (MPa)	$\tan \delta$ max ($^\circ\text{C}$)
PIL-CAN-IM	12.8	275	1.50	49.1
PIL-CAN-IM2	2.5	296	0.66	33.5

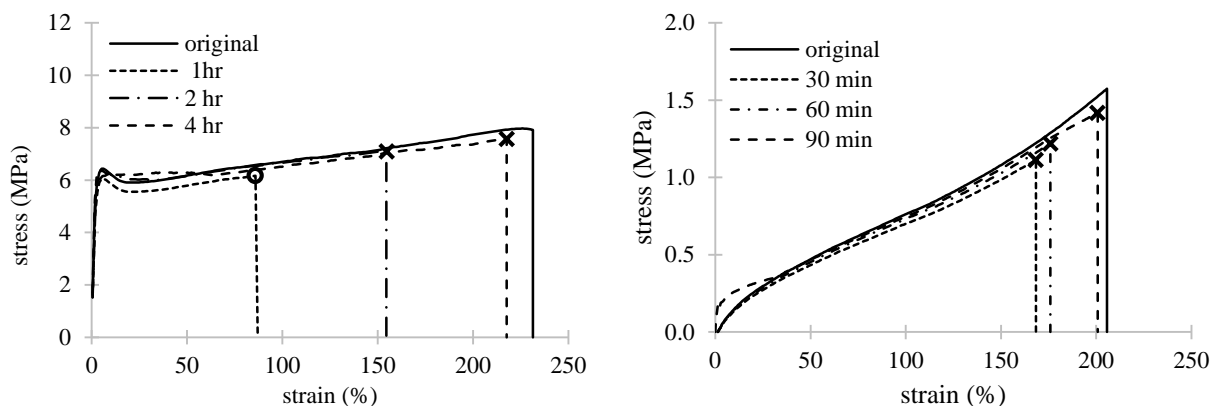


Figure 2.1: Stress-strain recovery data for (top) PIL-CAN-IM and (bottom) PIL-CAN-IM2 at 105 °C. Data points marked with an \circ represent breakage at the original healing point whereas points marked with an **X** represent breakage at a new point, away from the reheal point.

To test the ability of the polymers to exhibit recovery of mechanical stability, polymer films were first cut into thin strips and completely severed with a razor blade. The strips were overlapped and pressed down with finger pressure; the strips were then placed in an oven (105 °C) for various amounts of times under the weight of a 200g TeflonTM block for assurance of complete contact. Samples were taken out of the oven in different time intervals. The rehealed polymer strips underwent rehealing studies through use of dynamic mechanical analysis (DMA). Stress was recorded as a function of strain, and several samples exhibited new breaking points apart from its original cut. “Self-healing” occurred if a new break point was observed away from the original re-seal point with at least 70% recovery of the stress and strain at the break of the original (uncut) polymer. Note from **Figure 2.1** that PIL-CAN-IM exhibited “self-healing” after approximately 2 hours at 105 °C while PIL-CAN-IM2 re-healed within 30 minutes under the same conditions.

Figures 2.2 and **2.3** show pictures of representative samples after the tensile re-healing studies. Note that a new breaking point became more evident as samples were kept in the oven for

longer periods of time. Likewise, samples left in the oven for longer periods of time displayed new breaking points, points that are visibly different from the overlapping rehealed point.

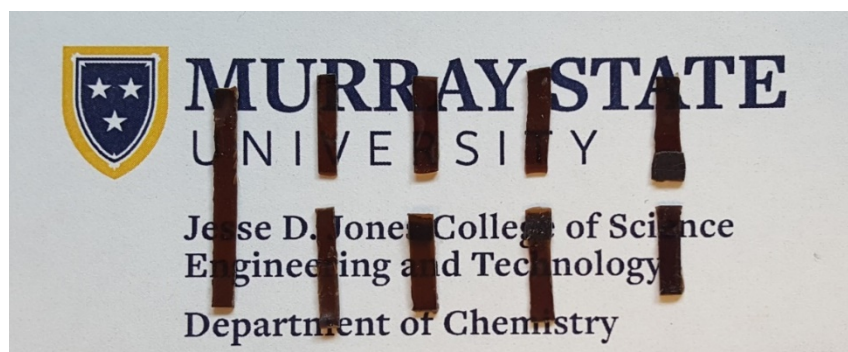


Figure 2.2: Samples from a representative re-heal stress-strain trial for PIL-CAN-IM at 105 °C. From left-to-right: original sample, freshly cut sample, 1 hr re-heal sample, 2 hr re-heal sample, 4 hr re-heal sample.



Figure 2.3: Samples from a representative re-heal stress-strain trial for PIL-CAN-IM2 at 105 °C. From left-to-right: original sample, freshly cut sample, 30 min re-heal sample, 60 min re-heal sample, 90 min re-heal sample.

2.3: Experimental

2.3.1: Materials

All chemicals were purchased from Sigma-Aldrich or Acros Organics and were used as received without further purification unless otherwise stated in the below procedures. An ELGA Purelab[®] Ultra filtration device produced ultrapure water having a resistivity of 18 M Ω -cm.

2.3.2: Synthesis of Mono-Imidazolium Maleimide [NTf₂] Monomer

Sodium imidazole (2.00 g, 0.0222 mol) was suspended in anhydrous THF (30 mL) under argon. Furan-protected *N*-(4-bromobutyl)maleimide **1** (6.34 g, 0.0211 mol) in anhydrous THF (70 mL) was added to the stirred solution dropwise via an addition funnel over a 30 minute period. The resulting mixture was heated to 60°C and held for 36 hours. For purification, the mixture was filtered and the solvent removed to give a yellow oil. The oil was partitioned between ethyl acetate and water, the organic phase removed, washed with brine, and dried over Na₂SO₄/MgSO₄. The product was filtered the solvent removed to give 5.04 g of a light yellow oil. ¹H NMR (400 MHz, DMSO-*d*₆, TMS): δ 7.53 (1 H, s, Im-*H*²), 7.07 (1 H, s, Im-*H*⁴), 6.82 (1 H, s, Im-*H*⁵), 6.51 (2 H, s, -CH=CH-), 5.08 (2 H, s, CH-O), 3.47 (2 H, t, *J* = 7.2 Hz, -CH₂-Im), 3.30 (2 H, t, *J* = 7.3 Hz, -CH₂-NC(O)), 2.88 (2 H, s, CH-C(O)N), 1.71 (2 H, m, -CH₂-CH₂-Im), 1.55 (2 H, m, -CH₂-CH₂-NC(O)). ¹³C NMR (100 MHz, DMSO-*d*₆, TMS): δ 176.27, 136.98, 136.12, 128.08, 118.91, 80.09, 46.82, 45.00, 36.87, 27.41, 23.59. Elem. Anal.: Calc. for C₁₅H₁₇N₃O₃: C, 62.7; H, 6.0; N, 14.6 %; Found: C, 62.4; H, 6.1; N, 14.8 %.

FUR-MA-imidazole **2** (1.00 g, 3.48 mmol) was dissolved in acetonitrile (20 mL). Furan-protected *N*-(4-bromobutyl)maleimide **1** (1.10 g, 3.66 mmol) was added to the solution, heated to 60°C and held for 24 hours. The solvent was removed under reduced pressure to give a light pink oil. Ethyl acetate (50 mL) was added to form a precipitate which was then isolated, washed with ethyl acetate (3 x 50 mL), dried under vacuum overnight to give 1.72 g of a light pink solid. ¹H NMR (400 MHz, DMSO-*d*₆, TMS): δ 9.27 (1 H, s, Im-*H*²), 7.82 (1 H, s, Im-*H*⁴), 7.74 (1 H, s, Im-*H*⁵), 6.55 (4 H, s, -CH=CH-), 5.11 (4 H, s, CH-O), 4.15 (4 H, m, -CH₂-Im), 3.35 (4 H, m, -CH₂-NC(O)), 2.92 (4 H, s, CH-C(O)N), 1.66-1.83 (4 H, m, -CH₂-CH₂-Im), 1.40 (2 H, m, -CH₂-NC(O)), 1.24 (2 H, m, -CH₂-CH₂-NC(O)). ¹³C NMR (100 MHz, DMSO-*d*₆, TMS): δ 176.65, 136.47,

136.02, 122.41, 80.37, 48.20, 47.16, 37.07, 26.48, 23.67. Elem. Anal.: Calc. for $C_{27}H_{31}BrN_4O_6$: C, 55.2; H, 5.3; N, 9.5 %; Found: C, 55.3; H, 5.2; N, 9.4 %.

FUR-MA-IM Br (1.05 g, 1.79 mmol) was dissolved in deionized water (15 mL). bis(trifluoromethanesulfonyl)imide (0.52 g, 1.82 mmol) in DI water (10 mL) was added to this stirred solution. A gummy precipitate was immediately formed to which dichloromethane (25 mL) was added to dissolve it. The resulting mixture was stirred at room temperature overnight, the organic phase removed and washed with DI water (3x15 mL). The product was dried under reduced pressure to give 1.32 g of a light pink oil. 1H NMR (400 MHz, $DMSO-d_6$, TMS): δ 9.11 (1 H, s, Im- H^2), 7.73 (2 H, s, Im- $H^{4,5}$), 6.55 (4 H, s, -CH=CH-), 5.11 (4 H, s, CH-O), 4.16 (4 H, m, -CH₂-Im), 3.35 (4 H, m, -CH₂-NC(O)), 2.91 (4 H, s, CH-C(O)N), 2.65-2.76 (4 H, m, -CH₂-CH₂-Im), 1.31-1.48 (4 H, m, -CH₂-CH₂-NC(O)). ^{13}C NMR (100 MHz, $DMSO-d_6$, TMS): δ 176.63, 136.46, 136.05, 122.45, 119.47 (q, $J = 321$ Hz, -CF₃), 80.38, 48.15, 47.14, 37.08, 26.47, 23.67. Elem. Anal.: Calc. for $C_{29}H_{31}F_6N_5O_{10}S_2$: C, 44.2; H, 4.0; N, 8.9 %; Found: C, 44.3; H, 3.9; N, 9.1 %.

FUR-MA-IM NTF₂ **4** (1.03g, 1.30 mmol) was dissolved in 1,1,2,2-tetrachloroethane (20 mL) in a 100-mL round-bottom flask equipped with a short path distillation head and collection flask. The stirred solution was heated to 120 °C and held for 24 hours. The solvent was removed under reduced pressure to give 0.81 g of a light yellow oil. 1H NMR (400 MHz, $DMSO-d_6$, TMS): δ 9.12 (1 H, s, Im- H^2), 7.76 (2 H, s, Im- $H^{4,5}$), 7.00 (4 H, s, -CH=CH-), 4.15 (4 H, m, -CH₂-Im), 3.40 (4 H, m, -CH₂-NC(O)), 1.73 (4 H, m, -CH₂-CH₂-Im), 1.45 (2 H, m, -CH₂-CH₂-NC(O)). ^{13}C NMR (100 MHz, $DMSO-d_6$, TMS): δ 171.13, 136.25, 134.53, 122.48, 119.50 (q, $J = 325$ Hz, -CF₃), 48.37, 36.33, 26.70, 24.73. Elem. Anal.: Calc. for $C_{21}H_{23}F_6N_5O_8S_2$: C, 38.7; H, 3.6; N, 10.8 %; Found: C, 38.5; H, 3.4; N, 10.6 %.

2.3.3: Synthesis of Bisimidazolium Maleimide [NTf₂] monomer

Furan-protected N-(4-bromobutyl)maleimide **1** (7.80 g, 25.0 mmol) and 1,1'-(1,6-hexanediyl)bisimidazole (2.70 g, 12.4 mmol) were dissolved in acetonitrile (100 mL). The solution was heated to 60°C for 48 hours, the residuals were removed under reduced pressure and washed with tetrahydrofuran (3x100 mL). Residuals were removed under high vacuum to give 8.47 g of light pink solid. ¹H NMR (400 MHz, DMSO-*d*₆, TMS): δ 9.28 (2 H, s, Im-*H*²), 7.82 (2 H, s, Im-*H*⁴), 7.76 (2 H, s, Im-*H*⁵), 6.53 (4 H, s, -CH=CH-), 5.09 (4 H, s, CH-O), 4.17 (8 H, m, -CH₂-Im), 3.36 (4 H, m, -CH₂-NC(O)), 2.91 (4 H, s, CH-C(O)N), 1.65-1.85 (8 H, m, -CH₂-CH₂-Im), 1.40 (4 H, m, -CH₂-CH₂-NC(O)), 1.24 (4 H, m, -CH₂-CH₂-CH₂-Im). ¹³C NMR (100 MHz, DMSO-*d*₆, TMS): δ 176.65, 136.46, 136.04, 122.54, 122.35, 80.37, 48.69, 48.18, 47.16, 37.10, 29.01, 26.54, 24.84, 23.69. Elem. Anal.: Calc. for C₃₆H₃₆Br₂N₆O₂: C, 52.8; H, 5.7; N, 10.3 %; Found: C, 53.1; H, 5.8; N, 10.1 %.

FUR-MA-IM2 Br salt (6.50 g, 7.94 mmol) was dissolved in DI water (80 mL). Lithium bis(trifluoromethylsulfonyl)imide (4.79 g, 16.7 mmol) was dissolved in DI water (40 mL) and added to the stirred solution; dichloromethane (100 mL) was added to aid in dissolution and mixing. The solution was stirred at room temperature for 24 hours, the organic phase separated and washed with DI water (3x75 mL). Volatiles were removed under reduced pressure to give 9.27 g of viscous light pink oil. ¹H NMR (400 MHz, DMSO-*d*₆, TMS): δ 9.09 (2 H, s, Im-*H*²), 7.73 (2 H, s, Im-*H*⁴), 7.70 (2 H, s, Im-*H*⁵), 6.51 (4 H, s, -CH=CH-), 5.08 (4 H, s, CH-O), 4.13 (8 H, m, -CH₂-Im), 3.34 (4 H, m, -CH₂-NC(O)), 2.88 (4 H, s, CH-C(O)N), 1.65-1.80 (8 H, m, -CH₂-CH₂-Im), 1.39 (4 H, m, -CH₂-CH₂-NC(O)), 1.22 (4 H, m, -CH₂-CH₂-CH₂-Im). ¹³C NMR (100 MHz, DMSO-*d*₆, TMS): δ 176.63, 136.46, 135.98, 122.53, 122.38, 119.75 (q, *J* = 323 Hz, -CF₃), 80.39,

48.79, 48.23, 37.07, 30.67, 29.05, 26.53, 24.94, 23.69. Elem. Anal.: Calc. for C₄₀H₄₃F₁₂N₈O₁₄S₄: C, 39.4; H, 3.8; N, 9.2 %; Found: C, 39.2; H, 4.0; N, 9.3 %.

FUR-MA-IM2 NTF₂ **5** (7.50g, 6.15 mmol) was dissolved in TCE (100 mL) in a 100-mL round-bottom flask equipped with a short path distillation head and collection flask. The stirred solution was heated to 120 °C and held for 24 hours. The solution was cooled to 50 °C and residual furan and TCE removed under high vacuum to give 6.52 g of viscous pink oil. ¹H NMR (400 MHz, DMSO-*d*₆, TMS): δ 9.12 (2 H, s, Im-*H*²), 7.76 (4 H, s, Im-*H*^{4,5}), 7.04 (4 H, s, -CH=CH-), 4.17 (8 H, m, -CH₂-Im), 3.41 (4 H, m, -CH₂-NC(O)), 1.71-1.84 (8 H, m, -CH₂-CH₂-Im), 1.41 (4 H, m, -CH₂-CH₂-NC(O)), 1.25 (4 H, m, -CH₂-CH₂-CH₂-Im). ¹³C NMR (100 MHz, DMSO-*d*₆, TMS): δ 171.14, 135.99, 134.55, 122.43, 119.46 (q, *J* = 320 Hz, -CF₃), 48.76, 48.42, 36.36, 29.06, 26.71, 24.95, 24.75. Elem. Anal.: Calc. for C₃₂H₃₈F₁₂N₈O₁₂S₄: C, 35.5; H, 3.5; N, 10.4 %; Found: C, 35.4; H, 3.4; N, 10.6 %.

2.3.4: Synthesis of PIL-CAN-IM/PIL-CAN-IM2

Resulting maleimide [NTf₂] monomers (3.00 mol eq.) from the previous syntheses were individually combined with TMPT-FUR (2.00 mol eq.) and stirred in acetonitrile at 60 °C to create the final product of PIL-CAN-IM and PIL-CAN-IM2, respectively.

2.3.5: Monomer Characterization

¹H and ¹³C NMR spectra were obtained on a JEOL-ECS 400 MHz spectrometer and reported chemical shift values were referenced to residual solvent signals (DMSO-*d*₆: ¹H, 2.50 ppm; ¹³C, 39.52 ppm). Elemental analyses (5 replicates for each polymer) were completed on a Perkin-Elmer 2400 CHNS/O Series II Elemental Analyzer. Residual bromide [Br] concentrations in monomers **4** and **7** were determined using ion chromatography (ICS-1100, Dionex) with an eluent concentration of 4.5 mN CO₃²⁻/1.4 mM HCO₃⁻ and a flow rate of 1.2 mL/min with a

suppressor current of 31 mA. Calibration with a set of aqueous standards prepared via serial dilution of a 1000 ppm [Br] stock solution (from sodium bromide, Aldrich, > 99.99 %). Each monomer was first dissolved in 1 mL of acetonitrile followed by injection. Residual [Br] was found to be less than 0.01 % w/w.

2.3.6: Polymer Characterization

Glass transition temperature (T_g) values were found using a TA Instruments Q200 Differential Scanning Calorimeter. T_g values were determined from the inflection point of the second heating event at a heating rate of 2 °C/min from 90 to 120 °C on 5-8 mg of sample. No change in T_g from the first to second heating was observed for any sample indicating that no annealing occurred as a result of the experimental conditions. A total of six replicate experiments were conducted for each PIL-CAN formulation), resulting in an error of ± 1.4 °C. Thermal stability is defined by $T_{d5\%}$, the temperature at which 5% mass loss was observed. $T_{d5\%}$ values were determined using a TA Instruments Q500 on 4-6 mg samples under nitrogen from 30-800 °C at a ramp rate of 10 °C/min. Triplicate experiments were run on each PIL-CAN formulation, resulting in an error of ± 2 °C.

Dynamic mechanical analysis (DMA) was utilized to determine elastic storage modulus (E') and tan delta curves, in film tension mode with a single frequency of 1 Hz and an amplitude of 1 μm at a heating rate of 5 °C/min from -50 to 125 °C. Tensile testing was also conducted using the TA Instruments Q800 DMA. Polymer samples were cut into rectangular strips and secured with the film clamps. The extension was increased at a rate of 20 mm/min at 25 °C until each sample broke. Evaluation of each PIL-CAN formulation was completed in triplicate, and reported stress and strain at break measurements were reported as an average.

2.3.7: Rehealing Studies

Determination of stress/strain recovery was completed as follows. Films were cut width wise with a razor blade to simulate a break point/fracture. The two cut ends were then overlapped by ~2 mm and were finger pressed together for several seconds. The materials were then placed in a convection oven at the desired temperature (105 °C) and removed at various time intervals for tensile testing. A 200 g Teflon™ block was placed gently on top of the samples to ensure that good contact was being made throughout the experiment. Stress and strain are reported for each sample at break point. Here, a polymer is defined as “self-healing” if a new break point was observed away from the original re-seal point with at least 70% recovery of the stress and strain at the break of the original (uncut) polymer. Tensile (stress/strain) testing was conducted as previous described.

2.4: Summary

Covalently-crosslinked networks are a vast class of elastic materials which retain their molecular structures though extensive covalent bonds found throughout the network. Though these structures are rigid, the application of various stresses can result in permanent deformation. These damages, however, may be reversed through the inclusion of dynamic covalent which allows for reshuffling of covalent bonds within the network. Networks, such as these, that can exhibit such rearrangements are known as covalent adaptable networks. A common type of dynamic covalent chemistry used in covalent adaptable networks is the ‘click-like’ Diels-Alder cycloaddition. Specifically, the furan and maleimide cycloadduct product which exhibits this dynamic nature. When thermally activated, this allows manipulation for rehealing abrasions, cracks and recycling through coupling the furan-maleimide linkage with the control at which the bond can be thermally activated.

The synthesis of self-healing polymers was achieved through imidazolium containing poly(ionic liquid) covalent adaptable networks. Recovery of mechanical and conductive properties were exhibited at levels exceeding 70% after two hours at 105°C and recovery up to 90% could be achieved over longer periods of time. DSC data showed a T_g of 12.8°C for PIL-CAN-IM and a T_g of 2.5° C for PIL-CAN-IM2. TGA yielded thermal stability values ($T_{d5\%}$) of 275°C for PIL-CAN-IM and 296°C for PIL-CAN-IM2.

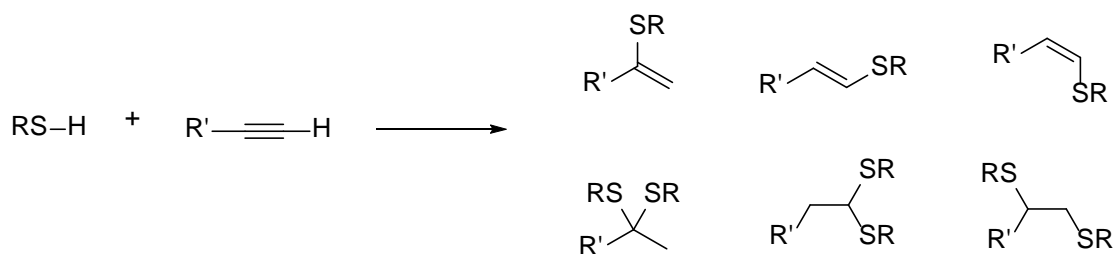
Chapter 3: Synthesis, Thermal and Mechanical Properties of Imidazolium Containing Thiol-yne Ionene Networks

3.1: Overview

As discussed in the opening chapter, thiol-ene photopolymerization represents an atom-efficient “click” approach (i.e. no byproducts) to creating covalently crosslinked ionene networks through the inclusion of ionic liquid groups in multifunctional ene monomers, wherein the network is formed upon exposure to a UV light source. Previous work with thiol-ene ionene networks in the Miller group has focused on imidazolium containing ene monomers in combination with a multifunctional thiol such as PTMP, or (pentaerythritol tetrakis (3-mercaptopropionate)).¹⁶ The cross-link density of these thiol-ene ionene networks was found to have a direct correlation to the IL group conductivity. In short, higher crosslink density led to lower ion mobility and thus lower conductivity.

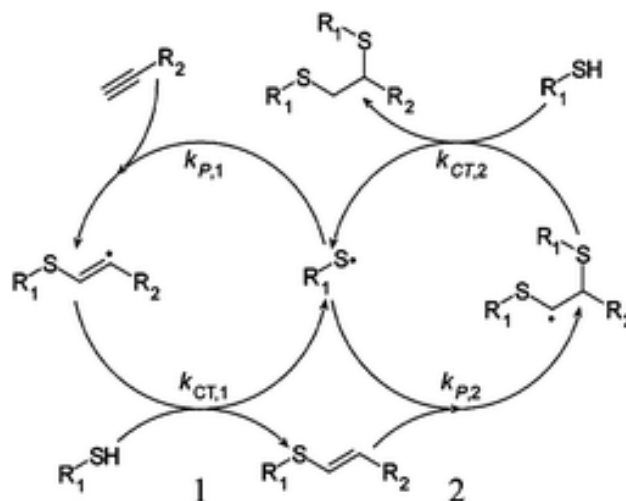
The results from these thiol-ene ionene network studies have led to further exploration into the effects of crosslink density on the properties of these networks. Alkyne functional monomers contain two π bonds, which can create hypercrosslinked networks. This should ultimately lead to a higher cross-link density; however, the true effect on ionic conductivity in thiol-yne systems is unknown. The proposed difference in the cross-link density between these two systems could be

attributed to the ability of the alkyne to react with two thiols. In a thiol-yne photoreaction, an alkyne terminated monomer is reacted with a thiol containing monomer. The monomer mixture, when combined with a photoinitiator, polymerizes upon exposure to a UV light source. This reaction proceeds as follows in **Scheme 3.1**, giving a mixture of vinyl sulfides and sulfides depending upon the functional group ratio of the original monomers (monitored by IR and NMR spectroscopy). If each monomer is multifunctional, polymer networks can be achieved with variable molecular weight and/or crosslink density.³²



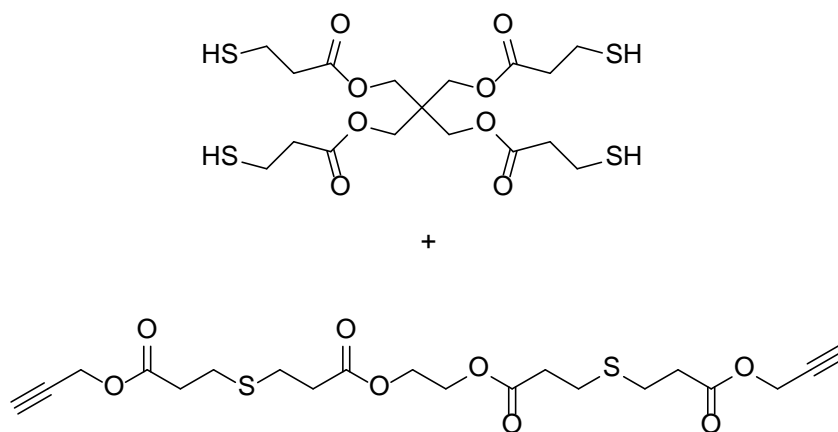
Scheme 3.1: Possible Products of a Thiol-yne Photoreaction.

The thiol-yne polymerization mechanism occurs via the addition of a thiyl radical to an alkyne group after the thiol undergoes hydrogen abstraction from an initiator fragment. The carbon centered radical resulting from this step then abstracts a hydrogen from another thiol, which forms a vinyl sulfide moiety, regenerating a thiyl radical. The regenerated thiyl radical then has the capability to undergo further reaction through the addition to a second pi bond or add to a new alkyne.³³ The radical addition mechanism through which this reaction proceeds is shown in **Scheme 3.2**.



Scheme 3.2: Radical Thiol-yne Reaction Mechanism.³⁴

Bowman and coworkers pioneered some of the initial thiol-yne photopolymerization reactions, an example of which is shown in **Scheme 3.3**. The reaction begins between an alkyne and a thiol group; combination of these two creates a vinyl sulfide. The vinyl sulfide consists of an alkene and a sulfide substituent. This alkene may then undergo another addition of a thiol, resulting in an alkane with two sulfide substituents. In the case of the thiol-yne polymerization shown in **Figure 3.3**, the highest T_g 's are observed in polymers that are stoichiometric (1:1 thiol: π bond functional group ratio). It is also noted that the T_g increases as the number of functional groups increases (i.e tri vs tetra functional); meaning a higher T_g corresponds to a higher cross-link density. A reverse trend in heat capacity is observed, making those higher cross-link densities reflect lower heat capacities at their respective T_g . Additionally, the storage modulus is dependent on the cross-link density; like T_g , the storage modulus increases with an increase in cross-link density (1.5-9.6 MPa).³³



Scheme 3.3: Example Thiol- and -Yne Monomer Combination.³⁴

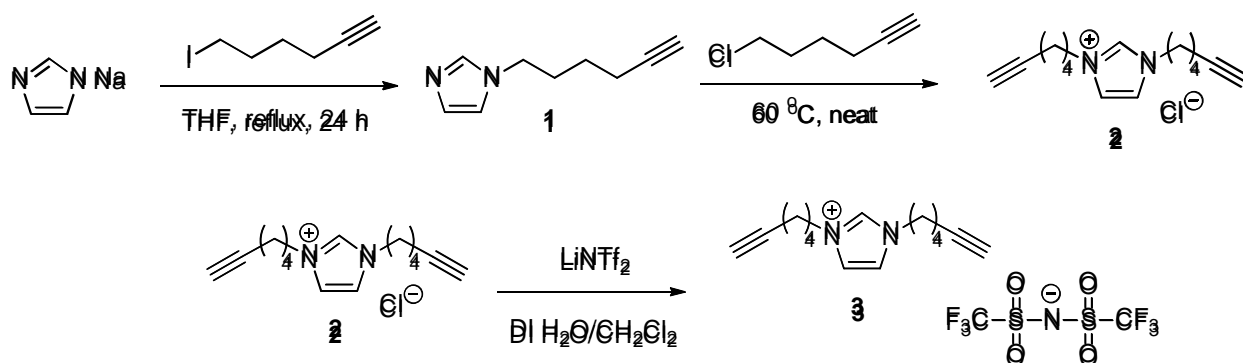
The effects of crosslink density on the mechanical and thermal properties of imidazolium-containing thiol-yne ionene networks will be explored throughout this chapter. Keeping at a constant number of functional groups in both the thiol (x4) and yne (x2) monomers but varying the functional group ratio and therefore the crosslink density of each polymer will give insight on the precise effects of crosslink density on the T_g and mechanical stability of the resulting ionene network.

3.2: Results and Discussion

3.2.1: Monomer Synthesis

6-Iodo-1-hexyne was synthesized using an S_N2 substitution approach, whereby 6-chloro-1-hexyne was reacted with sodium iodide in acetone. The isolated 6-iodo-1-hexyne was then reacted with sodium imidazole in tetrahydrofuran, resulting in *N*-(6-hexynyl) imidazole **1** after purification by column chromatography. Synthesis of bis(6-hexynyl)imidazolium was achieved by

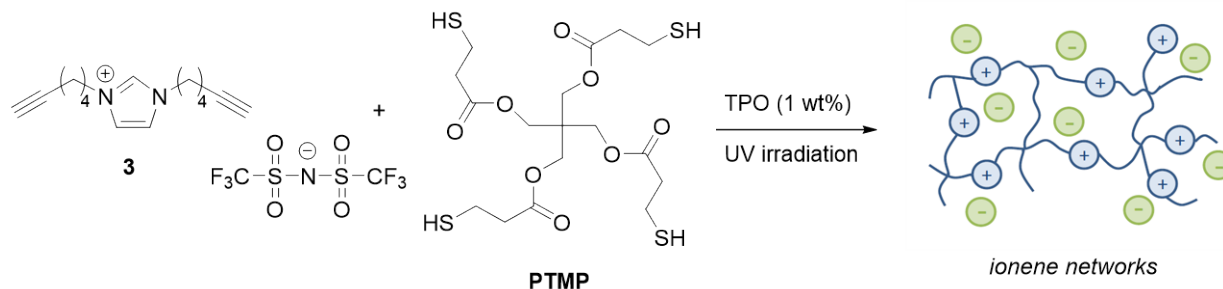
coupling *N*-(6-hexynyl) imidazole chloride **2** with an additional mole of 6-chloro-1-hexyne at 60 °C. An ion exchange reaction was then completed as the final step of this synthesis by reacting bis(6-hexynyl)imidazolium chloride **2** with and LiNTf₂ in DI H₂O, resulting in monomer **3**.



Scheme 3.4: Synthesis of Yne-functional [NTf₂] Monomer **3**.

3.2.2: Synthesis of Ionene Networks

The ionene networks were synthesized by dissolving TPO (diphenyl (2,4,6-trimethylbenzoyl phosphine oxide), a photoinitiator in PTMP. After dissolved, alkyne containing [NTf₂] anion monomer **3** was added and dissolved into solution. Varying amounts of each monomer were added for each polymerization to achieve a specific thiol:yne functional group ratio (2:1, 1.5:1, 1:1, 1:1.5, 1:2). Once in solution, the monomers were set aside in the dark to allow any bubbles to subside. The mixture was extracted from the vial using a syringe and slowly added to a mold created from two glass slides, a 500 μm Teflon spacer, and binder clips. The mold was then placed under a UV light for various times depending on the ratio (10-30 minutes), flipping halfway through. The synthesis of the ionene networks is shown below in **Scheme 3.5**.



Scheme 3.5: Synthesis of the Thiol-yne Ionene Networks.

3.2.3: Thermal properties:

The thermal properties of each network were evaluated by DSC (differential scanning calorimetry) and the T_g (glass transition temperature) values were found to be related to crosslink density. As seen in **Figure 3.1**, T_g was determined by the inflection point of each curve (second heating event). The 1:1 thiol:yne ratio is the stoichiometric functional group ratio. Here, the alkyne contributes 4 π bonds and the PTMP contributes 4 thiol groups. The 1:1 ratio provided the highest crosslink density, and therefore the highest T_g . Other reported T_g 's then decrease on either side of this value, respective to the off-stoichiometric ratios (**Table 3.1**). The decrease in T_g is more drastic in the polymers that have a higher ratio of -yne monomer.

Table 3.1: Glass Transitions Temperatures as determined by DSC

Ionene Network	T_g ($^{\circ}\text{C}$)	Ionene Network	T_g ($^{\circ}\text{C}$)
1-2 thiol-yne	-37.0	1.5-1 thiol-yne	-1.7
1-1.5 thiol-yne	-8.5	2-1 thiol-yne	-10.7
1-1 thiol-yne	4.2		

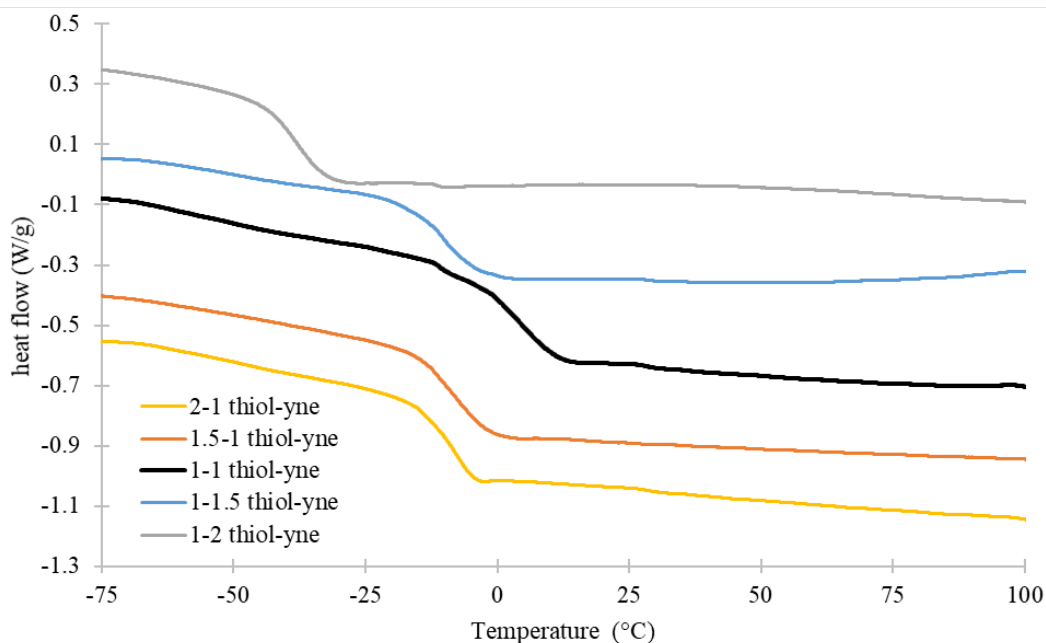


Figure 3.1: DSC Overlay of thiol-yne ionene networks.

3.2.4: Mechanical properties:

The storage modulus (E') is defined as a ratio of stress to strain. The data obtained by the DMA (dynamic mechanical analysis) shows the glassy region of the polymer, located in the lower temperature region, with the T_g is indicated by the inflection point of each curve (**Figure 3.2**). Above the T_g , the rubbery plateau region exists. The storage modulus is proportional to the crosslink density, where the 1:1 network again displayed the highest T_g and the highest E' value (7.15 MPa). Cross link density (ρ_x) is related to the storage modulus in a proportional manner, $\rho_x = \frac{E'}{3RT}$, meaning that a higher E' is also proportional to a higher cross link density.³⁶ The “DMA” T_g is more commonly determined by the peak of the $\tan \delta$ curve, which is a ratio of the loss modulus (E'') to the storage modulus (E'), where the precise “DMA” T_g is represented by the peak of this curve in **Figure 3.3**. A summary of the numerical mechanical properties can be found

in **Table 3.2**. E' values were found to be comparable (1.2-7.2 MPa) to similar thiol-ene networks (1.6-9.2 MPa) previously reported.³⁸ Thus, it appears from this initial series that the thiol-yne approach may not provide the proposed increase in crosslink density. In fact, crosslink densities of the thiol-yne networks were generally lower ($0.1-0.8 \times 10^{-4}$ mol/cm³) compared to thiol-ene networks ($1.7-9.9 \times 10^{-4}$ mol/cm³). Although more work is needed, we postulate that the vinyl sulfide that forms after the first addition may not be as reactive as expected due to steric bulk.

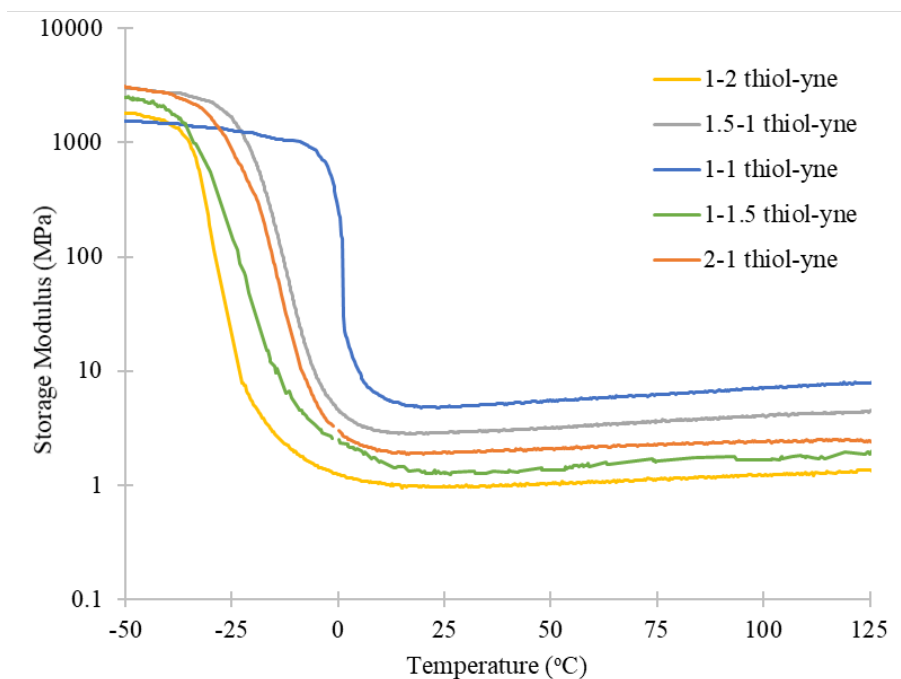


Figure 3.2: DMA Storage modulus curve overlay of thiol-yne ionene networks.

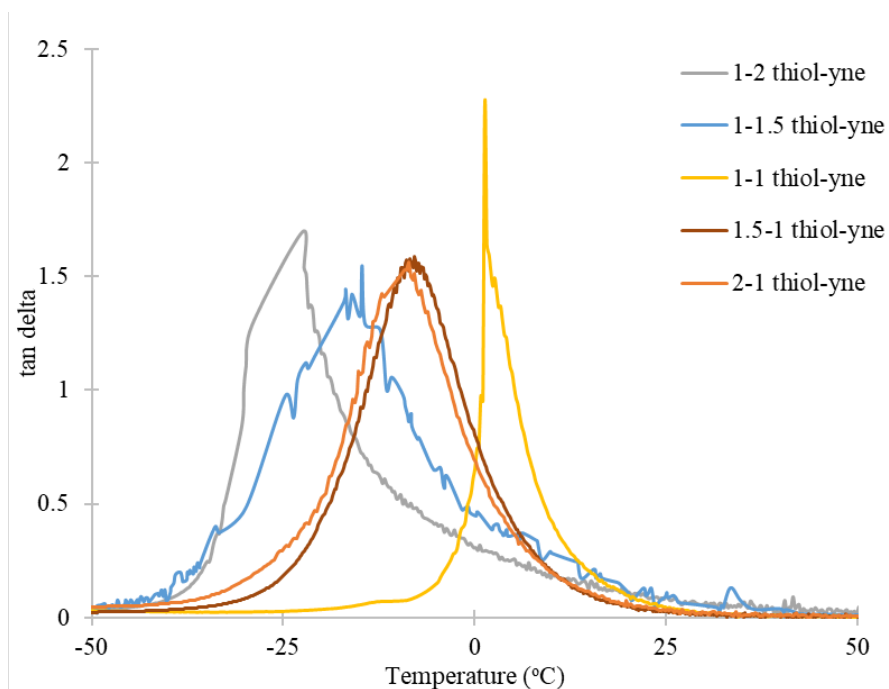


Figure 3.3: Tan δ Overlay of Thiol-yne Ionene Networks.

Table 3.2: Summary of Mechanical Properties of Thiol-yne Ionene Networks.

Ionene network	E' @ 100 °C (MPa)	$\tan \delta$ max (°C)	$\rho_x \times 10^{-4}$ (mol/cm ³)	Stress at break (MPa)	Strain at break (%)
1-2 thiol-yne	1.22	-22.5	0.131	0.38 ± 0.07	9.4 ± 0.5
1-1.5 thiol-yne	1.65	-15.8	0.177	0.65 ± 0.19	8.0 ± 1.0
1-1 thiol-yne	7.15	1.38	0.769	0.96 ± 0.06	5.9 ± 0.2
1.5-1 thiol-yne	4.12	-7.43	0.443	0.43 ± 0.08	6.7 ± 0.7
2-1 thiol-yne	2.41	-8.58	0.259	0.45 ± 0.04	9.3 ± 0.6

In addition to storage modulus evaluation, the ionene networks were also tested for stress (σ) and strain (ϵ) at break using the tensile testing option of the DMA. This test shows the polymer films have high mechanical stability which is proportional to their respective crosslink densities ($\sigma \cong \rho_x$). The polymers are capable of enduring high stress before breaking. However, their strain at break shows they are not elastic. Their elasticity, represented by strain ($\epsilon \cong \frac{1}{\rho_x}$), is inversely proportional to the cross-link density.

3.2.5: Photorheology

The gel point of any photopolymerization can be estimated rheologically from the crossover of the shear loss modulus (G'' , viscous component) and the shear storage modulus (G' , elastic component). In short, a sample of the monomer solution was placed on a quartz plate in the rheometer. A UV light guide was attached to the instrument, allowing for a UV beam to be shone through the bottom of the quartz plate, initiating polymerization. A top stainless steel plate was then lowered onto the sample until good contact was made. A “dead time” of 60-seconds was utilized before the UV lamp was turned on. Shown in **Figure 3.4** is an example of experimental data taken from the 1:1 thiol:yne monomer mixture. The approximate gel point from the G''/G' crossover point was determined to be 2.7 minutes. As shown in **Table 3.3**, The shortest time to gelation occurred when the maximum number of thiol and yne functional groups were present (i.e. the stoichiometric system). Longer gelation times were observed for the off-stoichiometric systems. These longer gelation times were also observed during the polymerization of samples used for the thermal and mechanical properties above wherein up to 20-30 minutes was needed for the mixtures that contained the most extreme excess of thiol or yne functional groups. These gelation times were significantly longer than analogous thiol-ene systems (<5 min).

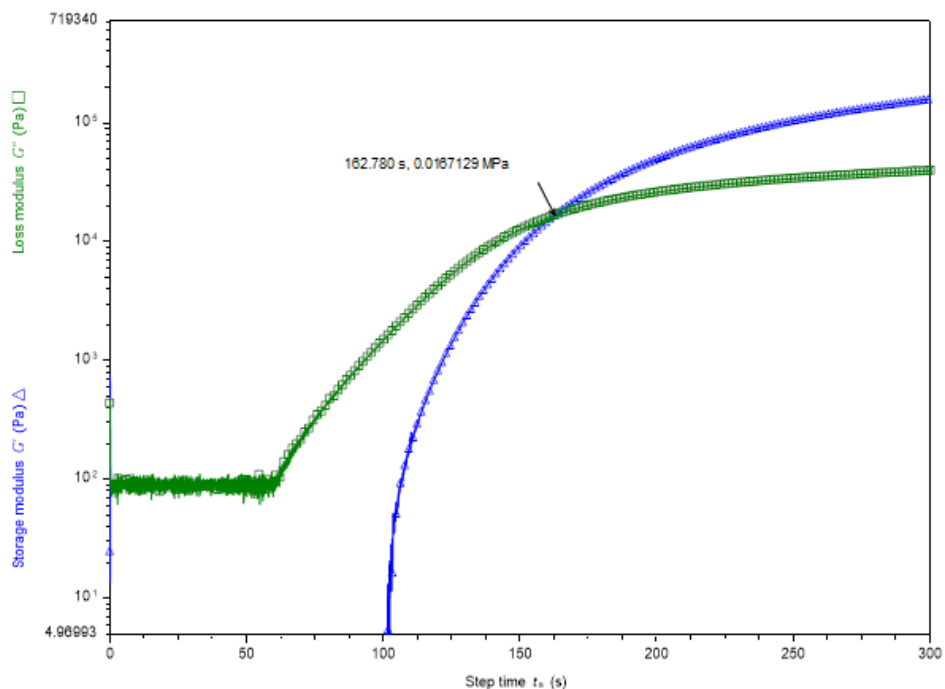


Figure 3.4: Sample Experimental Data from Photorheology of 1:1 Thiol:yne Ionene Network.

Table 3.3: Summary of Gelation Times for Thiol-yne Networks

Ionene network	p_c time (min)	Ionene Network	p_c time (min)
1-2 thiol-yne	4.27	1.5-1 thiol-yne	4.73
1-1.5 thiol-yne	3.93	2-1 thiol-yne	5.01
1-1 thiol-yne	2.72		

3.3: Experimental

3.3.1: General

All chemicals were purchased from Sigma-Aldrich or Acros Organics and were used as received without further purification unless otherwise stated in the below procedures. Pen-

taeythritol tetrakis(3-mercaptopropionate) (PTMP, >95%) was placed in a vacuum oven overnight before use. An ELGA Purelab® Ultra filtration device produced ultrapure water having a resistivity of 18 MΩ-cm. Synthesis of sodium imidazole has been previously reported.³⁸

3.3.2: Synthesis of 6-iodo-1-hexyne

Sodium iodide (32.59g, 0.2168 mol) was added to a 1-liter round bottom flask equipped with a magnetic stir bar and acetone (350 mL) was added. 6-Chloro-1-hexyne (12.675g, 0.1087 mol) was added and the mixture was stirred and heated to reflux overnight. The reaction was cooled to RT, filtered, washed with diethyl ether and the solvent removed under reduced pressure. To the slurry was added diethyl ether, filtered, and the solvent removed to give a crude orange oil. The crude product was purified by vacuum distillation at 33.0 mmHg, 75 °C – 85 °C, yielding a transparent pink oil (17.75g, 78.5%). ¹H NMR (400 MHz, CDCl₃, TMS): δ 3.181 (t, 2H, J=6.8 Hz), 2.198 (m, 2H, J=2.8 Hz), 1.946 (t, 1H, J=2 Hz), 1.916 (m, 2H, J=1.6 Hz), 1.610 (q, 2H, J=7.2 Hz).

3.3.3: Synthesis of *N*-(6-hexynyl) imidazole

Sodium imidazole (5.0 g, 0.0555 mol) was suspended in anhydrous THF (115 mL). 6-Iodo-1-hexyne (12.134 g, 0.0583 mol) was added and the mixture stirred for 1 hour at room temperature followed by heating at reflux for 24 hours. The rbf was cooled to room temperature, filtered, and the solvent removed under reduced pressure. The residue was then partitioned between dichloromethane and deionized water. The organic layer was isolated and washed with DI H₂O and brine. The organic layer was then dried over Na₂SO₄, filtered, and solvent removed. The product was purified by column chromatography (0-40% acetone in hexanes) to give a clear,

colorless oil (4.642 g, 56.4%). ^1H NMR (400 MHz, CDCl_3 , TMS): δ 3.88 (t, 2H, $J=7.32$ Hz), 2.12 (m, 2H, $J=2.76$ Hz), 1.89 (t, 1H, $J=2.0$ Hz), 1.81 (q, 2H, $J=8.0$ Hz), 1.42 (q, 2H, $J=8.0$ Hz).

3.3.4: Synthesis of bis(6-hexynyl)imidazolium chloride

N-(6-Hexynyl) imidazole (3.9 g, 0.0263 mol) and 6-chloro-1-hexyne (3.22 g, 0.0276 mol) were added to a 25 mL rbf equipped with a magnetic stir bar and stirred at 60°C for 48 hours. The product was broken up and vigorously washed with THF (30 mL). The supernatant liquid was pipetted off and the solid washed again with THF (30 mL); this process was repeated 3 times and the solvent was then removed under reduced pressure, resulting in a viscous dark yellow oil (6.44, 92%). ^1H NMR (400 MHz, $\text{DMSO}-d_6$, TMS): δ 9.20 (s, 1H), 7.79 9 (s, 2H) 4.18 (t, 4H, $J=7.2$ Hz), 2.82 (t, 1H, $J=1.6$ Hz), 2.20 (m, 4H, $J=2.8$ Hz), 1.85 (q, 4H, $J=8.0$ Hz), 1.41 (q, 4H, $J=8.0$ Hz).

3.3.5: Synthesis of bis(6-hexynyl)imidazolium [NTf_2]

Bis(6-hexynyl)imidazolium (2.0 g, 0.00755 mol) was dissolved in DI H_2O (20 mL) in a 250 mL rbf with a magnetic stir bar. In an Erlenmeyer flask, LiNTf_2 (2.277 g, 0.00793 mol) was dissolved in DI H_2O and added to the chloride solution. The mixture was capped and stirred at room temperature for 2 hours. The product was poured onto dichloromethane and the organic phase was washed with DI H_2O three times before the solvent was removed under reduced pressure. The product was then dried in the vacuum oven to remove residual solvent, resulting in a light yellow oil. ^1H NMR (400 MHz, $\text{DMSO}-d_6$, TMS): δ 9.19 (s, 1H), 7.79 9 (s, 2H) 4.18 (t, 4H, $J=7.2$ Hz), 2.49 (t, 1H, $J=1.6$ Hz), 2.21 (m, 4H, $J=2.8$ Hz), 2.19 (q, 4H, $J=8.0$ Hz), 1.41 (q, 4H, $J=8.0$ Hz). ^{13}C NMR (100 MHz, $\text{DMSO}-d_6$): δ 136.03, 122.49, 119.48 (t, $J=320$ Hz, $-\text{CF}_3$), 83.82, 71.63, 48.40, 28.51, 24.55, 17.13.

3.3.6: Polymer Synthesis

A total of five ionene networks were made for the functional group (thiol:yne) ratios of 2:1, 1.5:1, 1:1, 1:1.5, and 1:2. Each sample was prepared via the same process, with the amounts of each component as the variable. For the 1:1 network, TPO (13.7 mg, 0.03933 mmol) was dissolved in PTMP (0.671 g, 0.00205 mol) in a small vial. Bis(6-hexynyl)imidazolium [NTf₂] (0.70 g, 0.00136 mol) was added to the vial and dissolved. The vial was set aside in a dark space to allow any bubbles to subside. The monomer mixture was taken up in a 1 mL syringe and injected into the mold and placed under a UV light for 5 minutes. The mold was flipped and set for another 5 minutes.

3.3.7: Polymer Characterization

A TA instruments Q200 differential scanning calorimeter (DSC) was used to determine the glass transition temperature of each network. Samples ranging between 4-8 mg were run at a heating rate of 2 °C/min and run in duplicates and reported from the second heating event. A TA instruments Q800 dynamic mechanical analyzer (DMA) in film tension mode with a single frequency of 1 Hz and an amplitude of 1 μm at a heating rate of 5 °C/min was used to determine the mechanical properties of the network films. DMA experiments were run in duplicates and reported values reflect the second heating event. Stress/Strain tensile tests were also run on the samples but cutting rectangular strips from each polymer film and securing each end with the DMA clamps. The extension was increased at a rate of 20 mm/min at 25°C, with a preload force of 0.01 N until each sample broke. Each film was tested in triplicates and average values were reported.

3.4: Summary

Thiol-ene polymerizations represent an atom-efficient technique to create covalently crosslinked ionene networks through the inclusion of ILs into multifunctional ene monomers. Previous studies regarding the properties of thiol-ene monomers showed a strong correlation between the polymers crosslink density and their thermal, mechanical, and conductive properties. These results created an interest in exploring the properties of thiol-yne polymers to achieve higher crosslink densities, attributed to the two π bonds of an alkyne monomer. Thiol-yne polymers with variable molecular weights and crosslink density can be achieved by combining an alkyne terminated monomer, a thiol containing monomer, with a photoinitiator.

Thiol-yne polymers containing functional group ratios of 2:1, 1.5:1, 1:1, 1:1.5, 1:2 were created and analyzed for thermal and mechanical properties. Thermal analysis by differential scanning calorimetry revealed that the 1:1 ratio provided the highest glass transition temperature, due to its high crosslink density. T_g 's decrease on either side of the 1:1, with a more drastic decrease observed in the functional groups containing a greater amount of alkyne terminated monomer. This decline in T_g can also be contributed to the polymers crosslink density, which is lower in these films than those containing a greater amount of thiol monomer.

Mechanical analysis by dynamic mechanical analysis provides both thermal and mechanical properties on the polymers. A "DMA" T_g was determined through the ratio of the storage modulus (E') and the loss modulus (E'') giving a $\tan \delta$ curve, where the T_g is the peak of the resulting curve. The "DMA" T_g results concur with the DSC data that the 1:1 functional-group ratio reflects the highest T_g of 1.38 °C. The DMA also was used to analyze the crosslink density of each polymer. The 1:1 functional group ratio has a crosslink density (ρ_x) of 0.769×10^{-4} mol/cm³,

while the 1:2 functional group ratio has a crosslink density of 0.131×10^{-4} mol/cm³. This significantly lower density is reflected in the lowest T_g of -22.5 °C.

DMA was also used to determine mechanical stability by analyzing the films stress and strain at break. The films were found to possess high mechanical stability, reflected in the stress values (MPa). However, the low strain percentages reflect that the films are not flexible. Crosslink density again can be connected to this trend. Higher cross link densities films are stronger, reflected through a higher stress at break (0.96 MPa for 1:1 functional group ratio). The higher crosslink density films are also the least flexible (5.9%), whereas the lowest crosslink density film is the most flexible (9.4%).

REFERENCES

1. Yuan, J.; Mecerreyes, D.; Antonietti, M. Poly(ionic liquid)s: an update. *Prog. Polym. Sci.* **2013**, *38*, 1009-1036.
2. Qian, W.; Texter, J.; Yan, F. Frontiers in poly(ionic liquid)s: syntheses and applications. *Chem. Soc. Rev.* **2017**, *46*, 1124-1159.
3. Yuan, J.; Antonietti, M. Poly(ionic liquid)s: Polymers expanding classical property profiles. *Polymer* **2011**, *52*, 1469-1482.
4. Williams, S. R.; Long, T. E. Recent advances in the synthesis and structure-property relationships of ammonium ionenes. *Prog. Polym. Sci.* **2009**, *34*, 762-782.
5. Bara, J. E.; O'Harra, K. E. Recent advances in the design of ionenes: Toward convergence with high-performance polymers. *Macromol. Chem. Phys.* **2019**, *220*, 1900078.
6. O'Harra, K. E.; Bara, J. E. Toward controlled functional sequencing and hierarchical structuring in imidazolium ionenes. *Polym. Int.* **2020**, *in press*. <https://doi.org/10.1002/pi.6109>
7. Choi, U. H.; Lee, M.; Wang, S.; Liu, W.; Winey, K. I.; Gibson, H. W.; Colby, R. H. Ionic conduction and dielectric response of poly(imidazolium acrylate) ionomers. *Macromolecules* **2012**, *45*, 3974-3985.
8. Lee, M.; Choi, U. H.; Colby, R. H.; Gibson, H. W. Ion conduction in imidazolium acrylate ionic liquids and their polymers. *Chem. Mater.* **2010**, *22*, 5814-5822.
9. Fan, F.; Wang, Y.; Hong, T.; Heres, M. F.; Saito, T.; Sokolov, A. P. Ion conduction in polymerized ionic liquids with different pendant groups. *Macromolecules* **2015**, *48*, 4461-4470.

10. Choi, J. -H.; Ye, Y.; Elabd, Y. A.; Winey, K. I. Network structure and strong microphase separation for high ion conductivity in polymerized ionic liquid block copolymers. *Macromolecules* **2013**, *46*, 5290-5300.
11. Meek, K. M.; Elabd, Y. A. Polymerized ionic liquid block copolymers for electrochemical energy. *J. Mater. Chem. A* **2015**, *3*, 24187-24194.
12. Williams, S. R.; Salas-de la Cruz, D.; Winey, K. I.; Long, T. E. Ionene segmented block copolymers containing imidazolium cations: Structure-property relationships as a function of hard segment content. *Polymer* **2010**, *51*, 1252-1257.
13. Kim, S.; Miller, K. M. Synthesis and thermal analysis of crosslinked imidazolium-containing polyester networks prepared by Michael addition polymerization. *Polymer* **2012**, *53*, 5666-5674.
14. Tracy, C. A.; Adler, A. M.; Nguyen, A.; Johnson, R. D.; Miller, K. M. Covalently crosslinked 1,2,3-triazolium-containing polyester networks: Thermal, mechanical and conductive properties. *ACS Omega* **2018**, *3*, 13442-13453.
15. Rhoades, T. C.; Wistrom, J. C.; Johnson, R. D.; Miller, K. M. Thermal, mechanical and conductive properties of imidazolium-containing thiol-ene poly(ionic liquid) networks. *Polymer* **2016**, *100*, 1-9.
16. Bratton, A. F.; Kim, S.; Ellison, C. J.; Miller, K. M. Thermomechanical and conductive properties of thiol-ene poly(ionic liquid) networks containing backbone and pendant imidazolium groups. *Ind. Eng. Chem. Res.* **2018**, *57*, 16526-16536.

17. McBride, M. K.; Brady, W. T.; Brown, T.; Cox, L. M.; Sowan, N.; Wang, C.; Podgorski, M.; Martinez, A. M.; Bowman, C. N. Enabling applications of covalent adaptable networks. *Annu. Rev. Chem. Biomol. Eng.* **2019**, *10*, 175-98
18. Jin, Y.; Yu, C.; Denman, R. J.; Zeng, W. Recent advances in dynamic covalent chemistry. *Chem. Soc. Rev.* **2013**, *42*, 6634.
19. Chakma, P.; Konkolewicz, D. Dynamic covalent bonds in polymeric materials. *Angew. Chem. Int. Ed.* **2019**, *58*, 9682-9695.
20. Kloxin, C. J.; Bowman, C. N. Covalent adaptable networks: smart, reconfigurable and responsive network systems. *Chem. Soc. Rev.* **2013**, *42*, 7161.
21. Kloxin, C. J.; Scott, T. F.; Adzime, B. J.; Bowman, C. N. Covalent Adaptable Networks (CANs): A unique paradigm in cross-linked polymers. *Macromolecules* **2010**, *43*, 2643-2653.
22. Adzima, B. J.; Aguirre, H. A.; Kloxin, C. J.; Scott, T. F.; Bowman, C. N. Rheological and chemical analysis of reverse gelation in a covalently cross-linked Diels-Alder polymer Networks. *Macromolecules* **2008**, *41*, 9112-9117.
23. Craven J. M. Cross-linked thermally reversible polymers produced from condensation polymers with pendant furan groups cross-linked with maleimides. DuPont, *US Pat*, 3435003, 1969.
24. Chen, X.; Dam, M. A.; Ono, K.; Mal, A.; Shen, H.; Nutt, S. R.; Sheran, K.; Wud, F. A thermally re-mendable cross-linked polymeric material. *Science*, **2002**, *295*, 1698.
25. Imai, Y.; Itoh, H.; Naka, K.; Chujo, Y. Reversible gelation of polyoxazoline by means of Diels-Alder reaction. *Macromolecules* **2000**, *33*, 4343.
26. Inoue, K.; Yamashiro, M.; Iji, M. Design of melt-recyclable poly(ϵ -caprolactone)-based supramolecular shape-memory nonocomposites. *J. Appl. Polym. Sci.* **2009**, *112*, 876.

27. Yang, K.; Grant, J. C.; Lamey, P.; Joshi-Imre, A.; Lund, B. R.; Smaldone, R. A.; Voit, W. Diels-Alder reversible thermoset 3D printing: isotropic thermoset polymers via fused filament fabrication. *Adv. Funct. Mater.* **2017**, *27*, 1700318.
28. Jin, K.; Kim, J.; Xu, J.; Bates, F. S.; Ellison, C. J. Melt-blown cross-linked fibers from thermally reversible Diels-Alder polymer networks. *ACS Macro Lett.* **2018**, *7*, 1339.
29. Yuan, J.; Antonietti, M. Poly(ionic liquid)s: polymers expanding classical property profiles. *Polymer* **2014**, *52*, 1469.
30. Lindenmeyer, K. M.; Johnson, D. R.; Miller, K. M. Self-healing behavior of furan-maleimide poly(ionic liquid) covalent adaptable networks. *Polymer Chemistry.* **2020**, *11*, 5321-5326.
31. Rao, V.; Navath, S.; Kottur, M.; McElhanon, J. R.; McGrath, D. V. An efficient reverse Diels-Alder approach for the synthesis of N-alkyl bismaleimides. *Tetrahedron Letters* **2013**, *54*, 5011-5013.
32. Lowe, A.B. Thiol-yne 'click'/coupling chemistry and recent applications in polymer and materials synthesis and modification. *Polymer.* **2014**, *55*, 5517-5549.
33. Fairbanks, B.D.; Scott, T.F.; Kloxin, C.J.; Anseth, K.S.; Bowman, C.N. Thiol-yne Photopolymerizations: Novel mechanism, kinetics, and step-growth formation of highly cross-linked networks. *Macromolecules.* **2009**, *42*, 211-217.
34. Chan, J.W.; Shin, J.; Hoyle, C.E.; Bowman, C.N.; Lowe, A.B. Synthesis, thiol-yne "click" photopolymerization of networks derived from novel multifunctional alkynes. *Macromolecules.* **2010**, *43*, 4937-4942.
35. Mather, B.D.; Miller, K.M.; Long, T.E. Novel Michael addition networks containing Poly(propylene glycol) telechelic oligomers. *Macromol. Chem. Phys.* **2006**, *207*, 1324-1333.

36. Bontrager, N.C.; Radomski, S.; Daymon, S.P.; Johnson, D.; Miller, K.M. Influence of counteranion and humidity on the thermal, mechanical and conductive properties of covalently crosslinked ionenes. *Polymer*. **2021**, *222*, 123641.

37. Bara, J.E. Versatile and scalable method for producing *N*-functionalized imidazoles. *Ind. Eng. Chem. Res.* **2011**, *50*, 13614-13619.

Supplementary Information

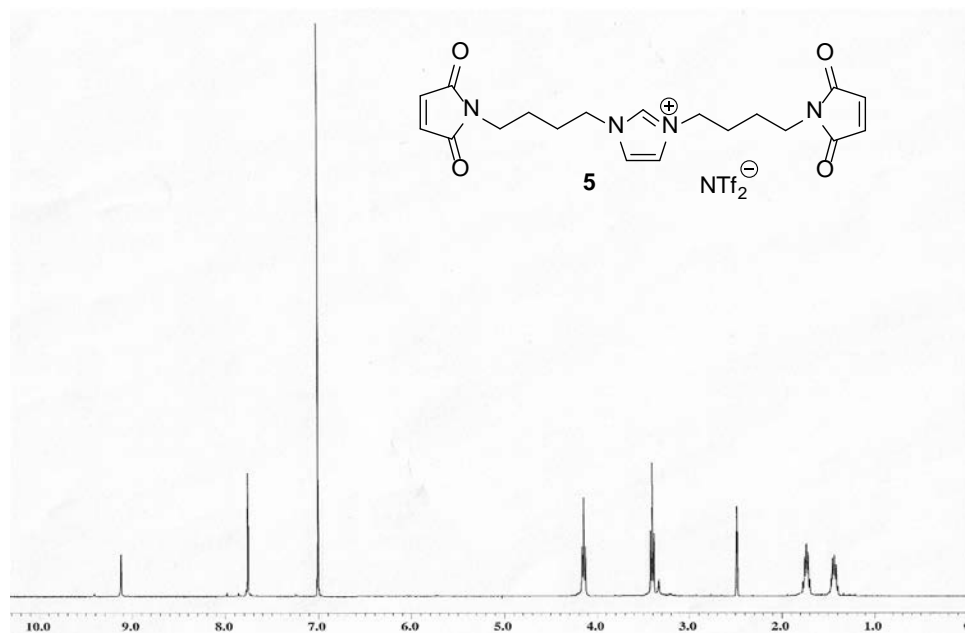


Figure S1: ¹H NMR spectrum of MA-IM NTf₂ 5 (DMSO-*d*₆).

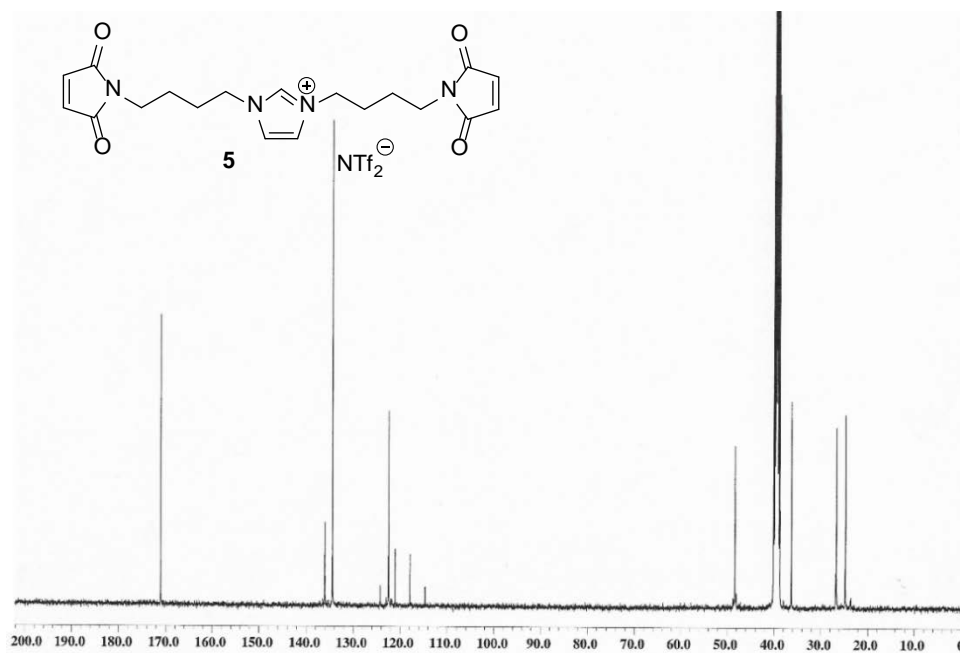


Figure S2: ¹³C NMR spectrum of MA-IM NTf₂ 5 (DMSO-*d*₆).

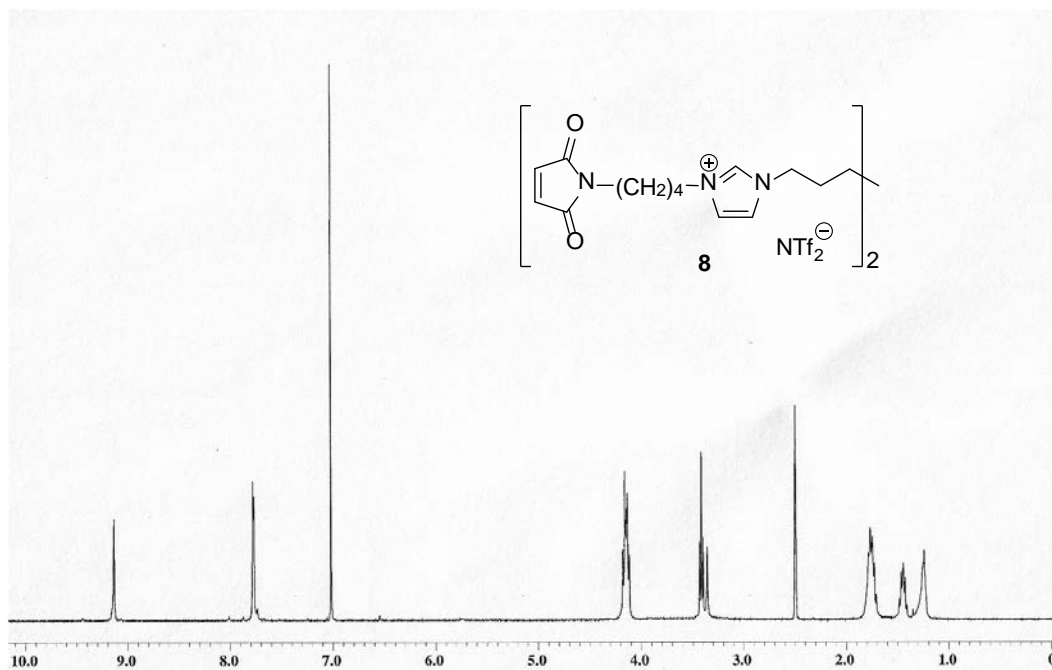


Figure S3: ¹H NMR spectrum of MA-IM2 NTf₂ 8 (DMSO-*d*₆).

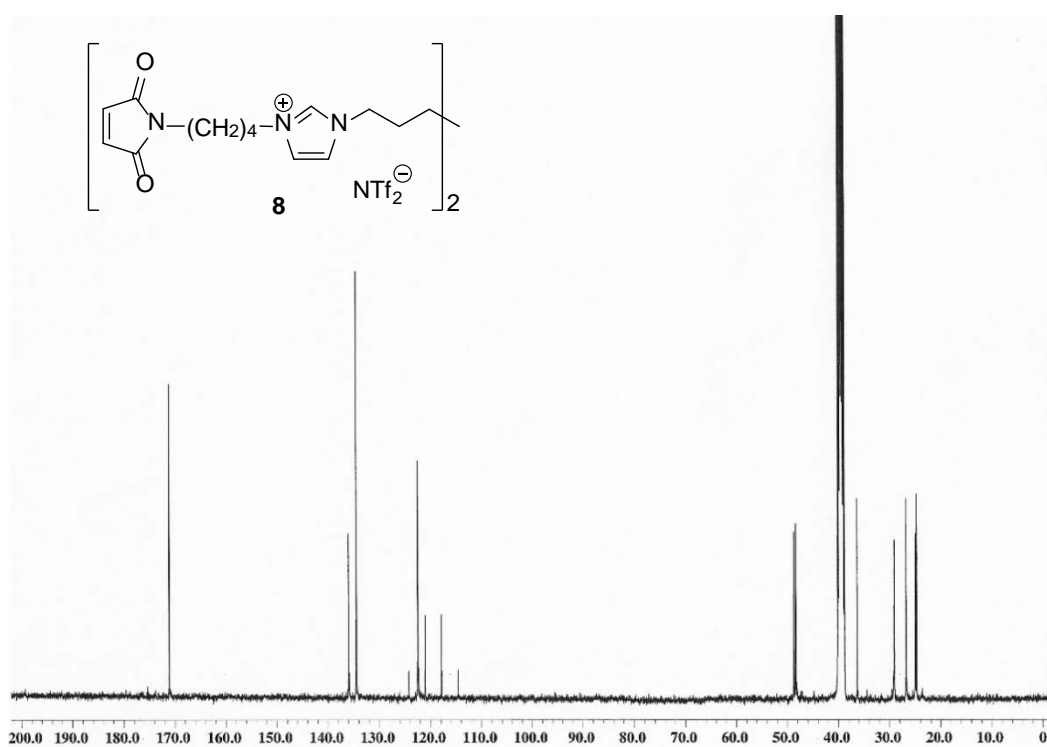


Figure S4: ¹³C NMR spectrum of MA-IM2 NTf₂ 8 (DMSO-*d*₆).

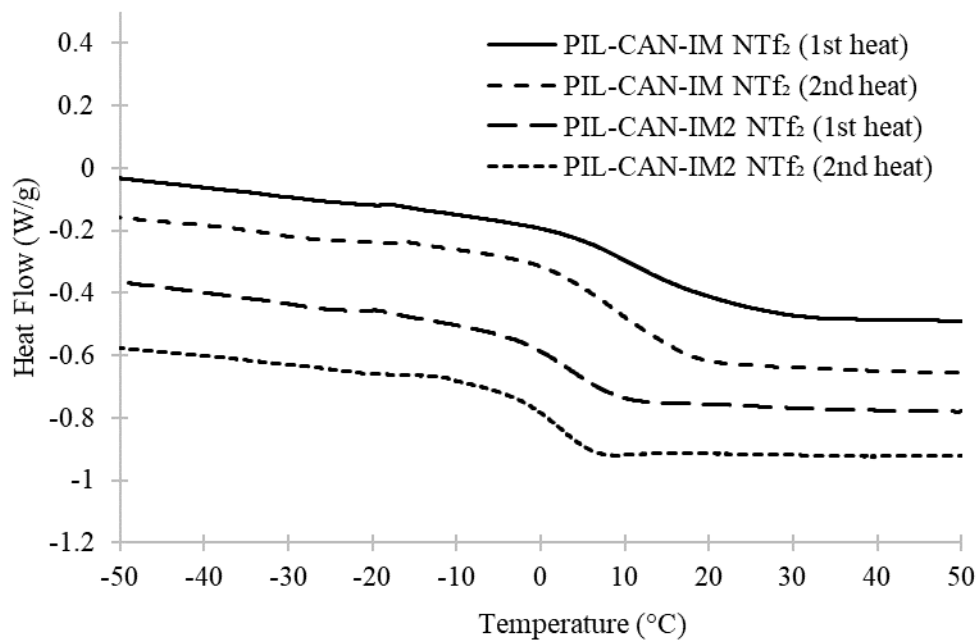


Figure S5: Overlay of DSC traces (1st and 2nd heating) for PIL-CAN-IM and PIL-CAN-IM2 networks.

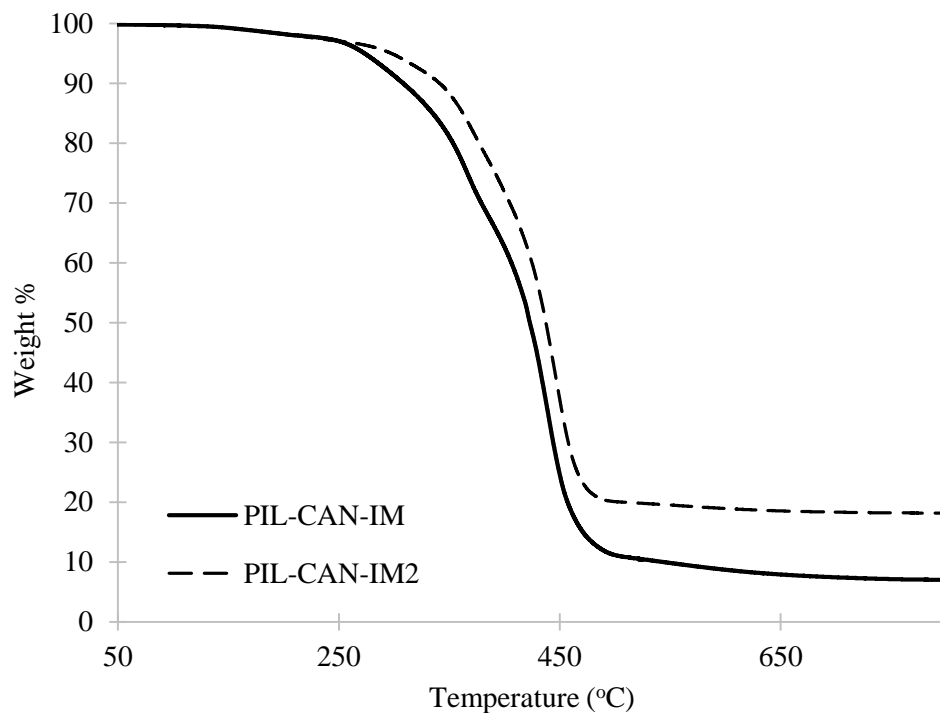


Figure S6: Overlay of TGA traces for PIL-CAN-IM and PIL-CAN-IM2 networks.

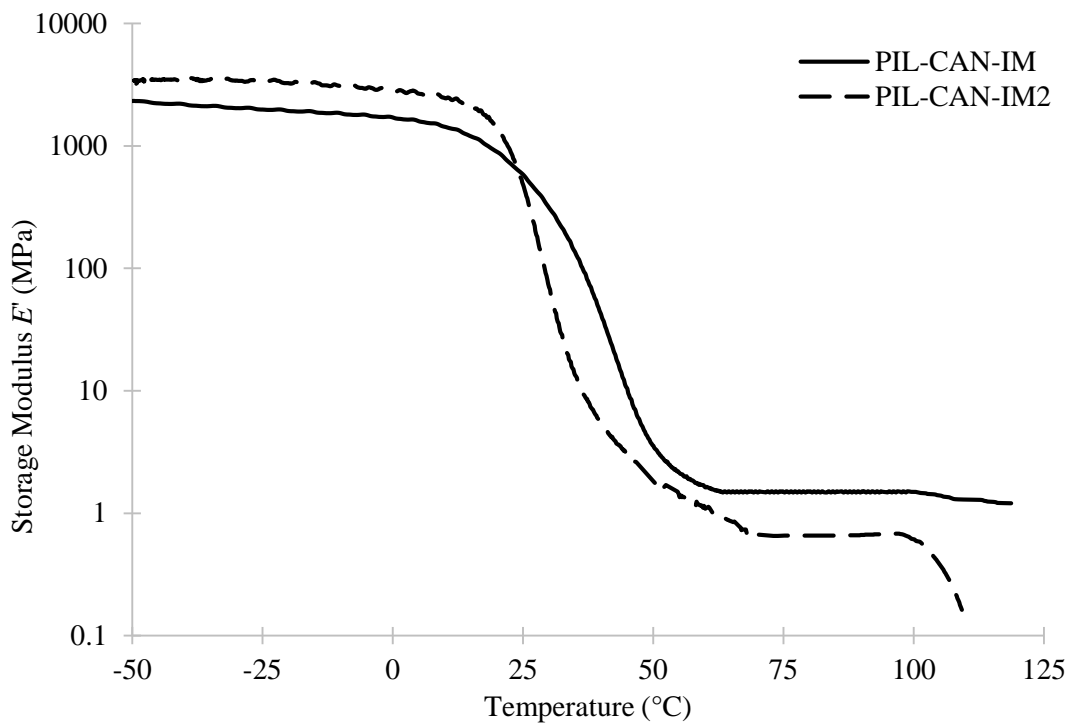


Figure S7: Overlay of DMA curves for PIL-CAN-IM and PIL-CAN-IM2 networks.

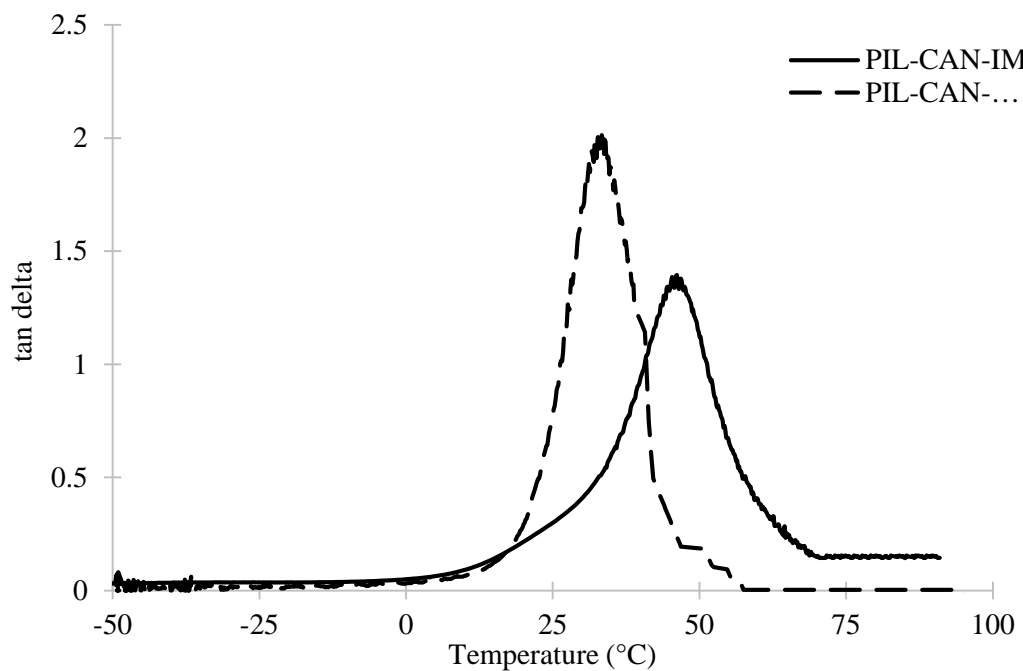


Figure S8: Overlay of $\tan \delta$ curves for PIL-CAN-IM and PIL-CAN-IM2.

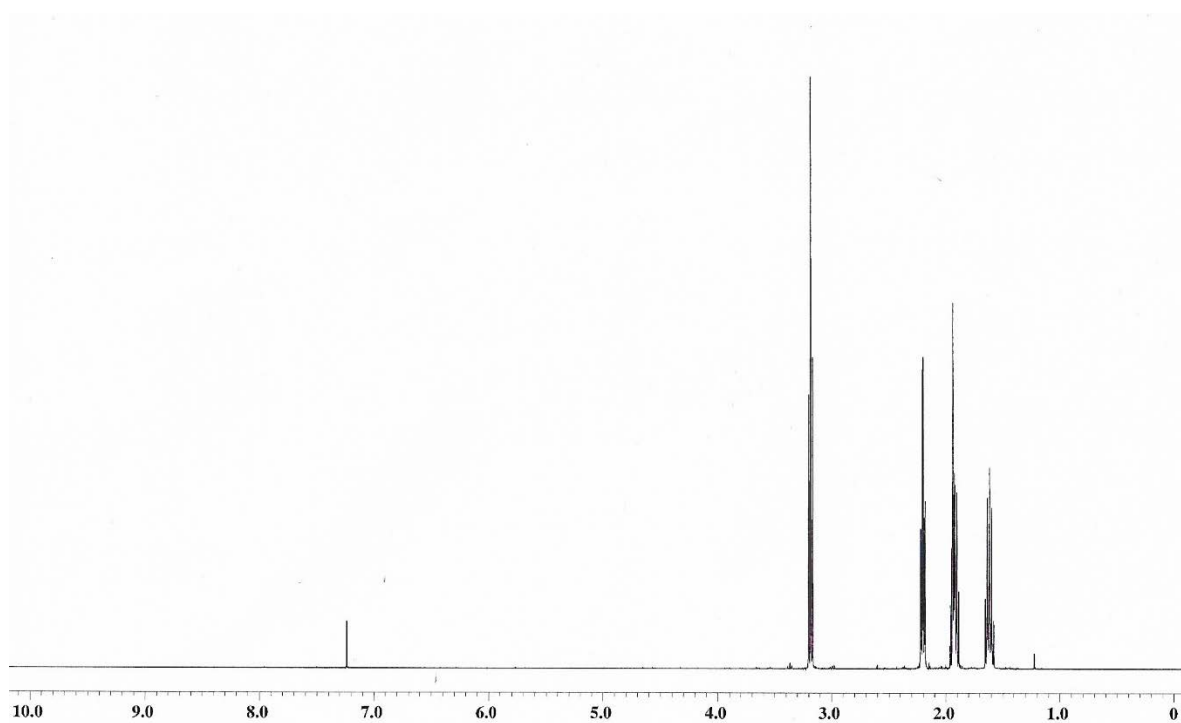


Figure S9: ^1H NMR spectrum of 6-iodohex-1-yne (CDCl_3).

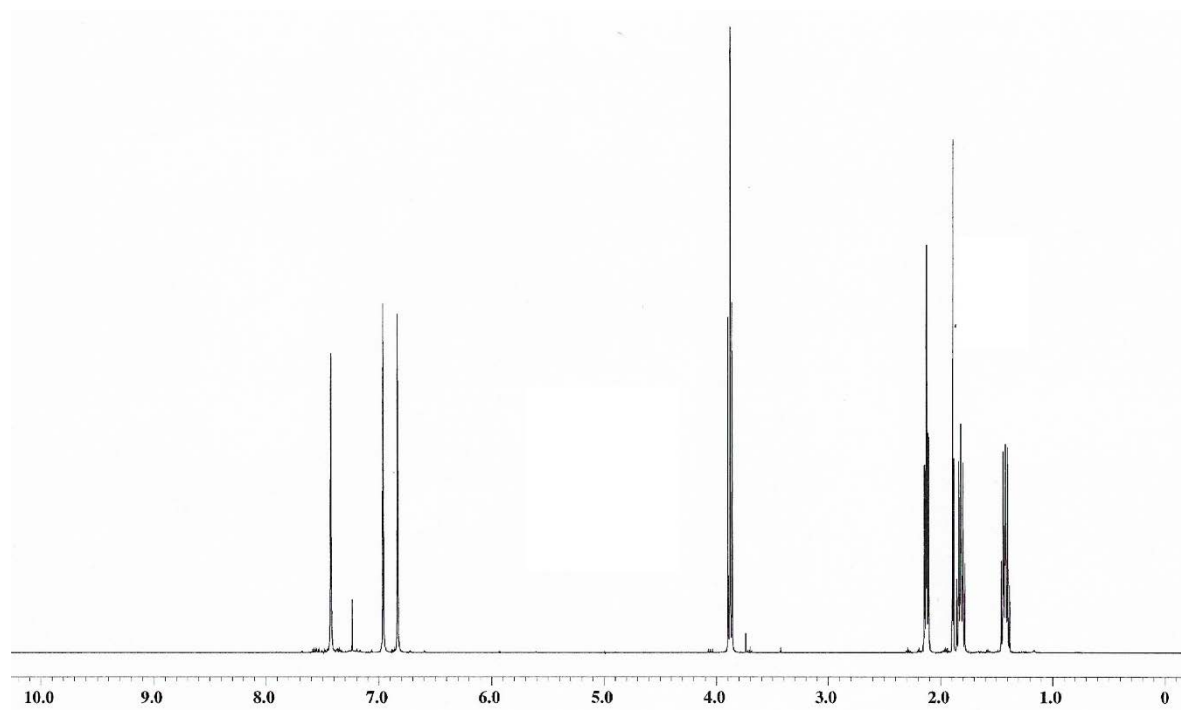


Figure S10: ^1H NMR spectrum of 6-hexynylimidazole (CDCl_3).

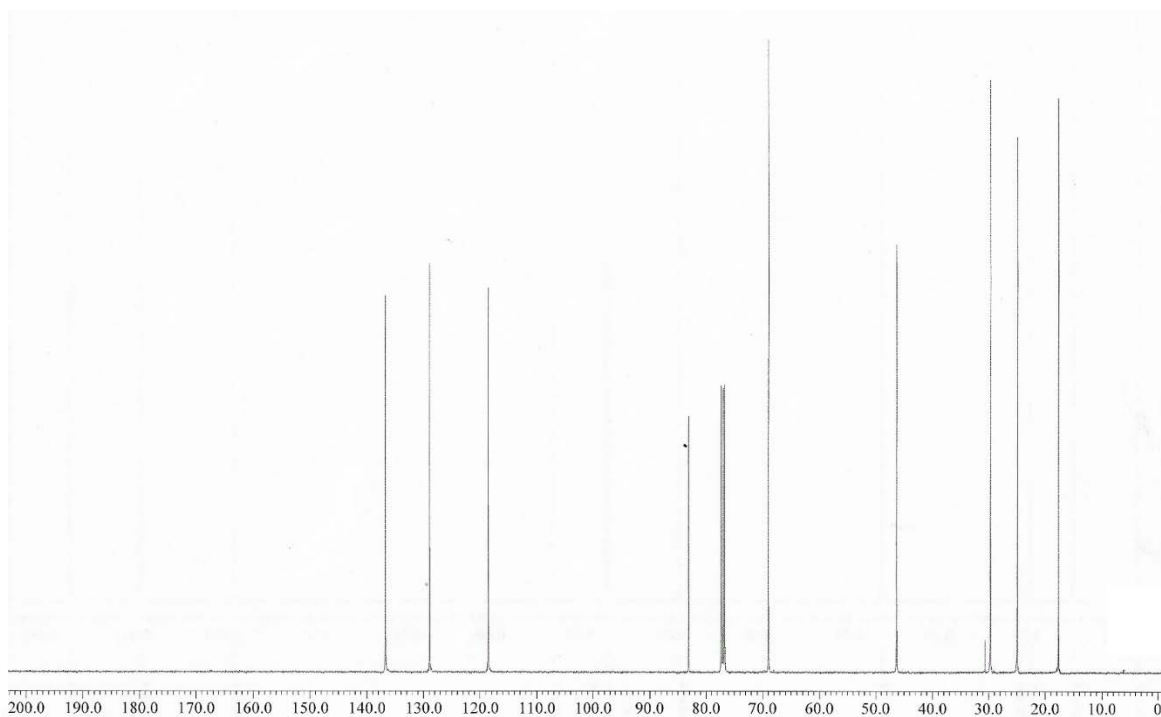


Figure S11: ^{13}C NMR spectrum of 6-hexynylimidazole (CDCl_3).

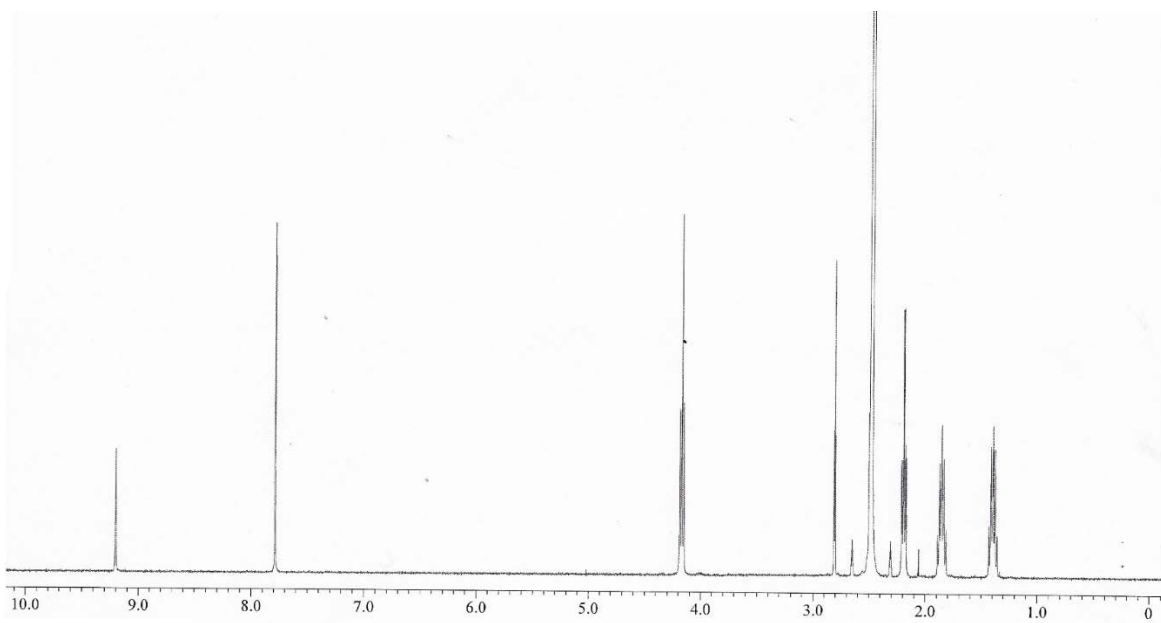


Figure S12: ^1H NMR spectrum of bis(6-hexynyl)imidazolium chloride ($\text{DMSO}-d_6$).

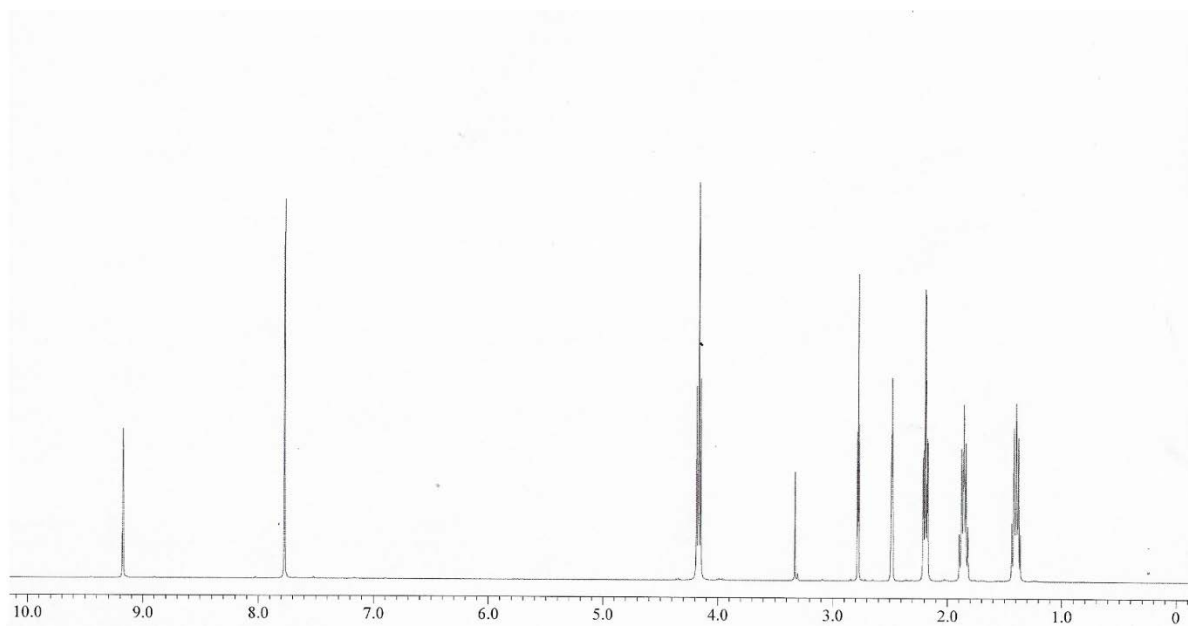


Figure S13: ^1H NMR spectrum of bis(6-hexynyl)imidazolium [NTf_2] ($\text{DMSO-}d_6$).

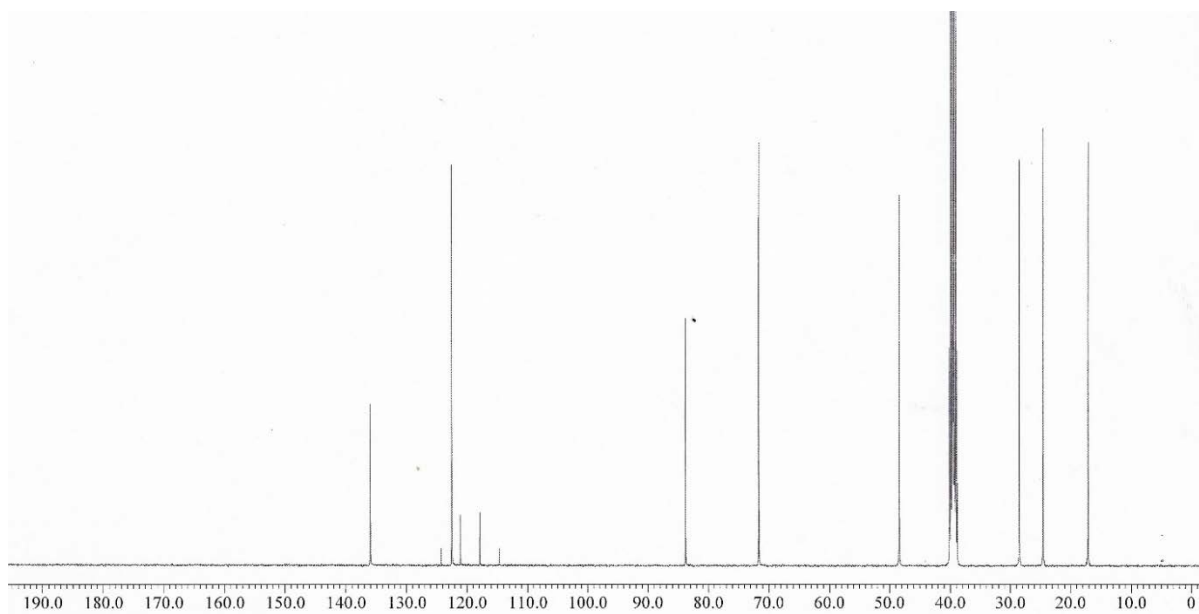


Figure S14: ^{13}C NMR spectrum of bis(6-hexynyl)imidazolium [NTf_2] ($\text{DMSO-}d_6$).